1971

Phase equilibrium and thermodynamic study of lime-iron oxide solid solutions

Shin Suk Kang

PHASE EQUILIBRIUM AND THERMODYNAMIC STUDY OF LIME-IRON OXIDE SOLID SOLUTIONS

BY

SHIN SUK KANG, 1938-

A THESIS

Presented to the Faculty of the Graduate School of the

UNIVERSITY OF MISSOURI-ROLLA

In Partial Fulfillment of the Requirements for the Degree

MASTER OF SCIENCE IN METALLURGICAL ENGINEERING

1971

Approved by

A. R. Mones (Advisor) Fred Kissinger

Charles A Sorrell

ABSTRACT

The solubility limits of iron oxide in solid lime were determined as a function of oxygen pressure at 1300° and 1400°C in the system CaO-iron oxide. The stability region of dicalcium ferrite was determined with respect to formation of lime-iron oxide solid solution and liquid oxide. In addition, the hydration behavior in moist air of pure lime and sintered mixtures of lime and iron oxide was also observed.

Pelletized samples were equilibrated under known oxygen partial pressures and quenched. Phases present in the quenched samples were identified by microscopy.

The solubility limit of iron oxide in CaO is strongly dependent on the oxygen partial pressure, and decreases with increasing temperature. On the basis of these results, isothermal sections of the CaO-rich portion of the system CaO-iron oxide were constructed at 1300° and 1400°C. Hydration tests on pure lime and CaO-iron oxide mixtures showed that lime containing iron oxide is more resistant to hydration than pure lime. The largest resistance to hydration was achieved by a lime solid solution saturated with iron oxide.

ACKNOWLEDGEMENTS

The author wishes to express his sincere gratitude to his advisor, Dr. Arthur E. Morris, for his invaluable guidance throughout the course of this study.

The financial support of the National Lime Association is gratefully acknowledged.

TABLE OF CONTENTS

LIST OF FIGURES

LIST OF TABLES

LIST OF SYMBOLS AND ABBREVIATIONS

BOF	Basic oxygen furnace
CaO(ss)	CaO-rich CaO-iron oxide solid solution
C_2F or $2CaO \cdot Fe_2O_3$	Dicalcium ferrite (stoichiometric)
CF	Monocalcium ferrite
CF_2	Calcium diferrite
CW	Calciowustite
FeO	Hypothetical stoichiometric wustite
"FeO" or FeO_n	Total iron oxide expressed as FeO
"FeO"(ss)	"FeO"-rich CaO-iron oxide solid solution
H	Hematite
Liq. or L	Liquid oxide
M	Magnetite
(m)	Minor amount (~10%) of the indicated phase
$N_{"FeO"}$	Mole fraction of "FeO"
pO_2	Partial pressure of oxygen
(ss)	Solid solution
(tr)	A trace amount (~1%) of the indicated phase

I. INTRODUCTION

In the conventional basic open hearth steelmaking process, the main fluxing and refining material used has been limestone. But the newer and more recently developed basic oxygen furnace (BOF) steelmaking process requires the addition of lime as a flux. The three main reasons for this are first, that the characteristic fast reaction between gaseous oxygen and hot metal does not allow time for calcination of limestone before it can be dissolved. Second, limestone has a tendency to cause excessive turbulence in the bath, leading to ejection of slag and metallics from the furnace mouth as calcination proceeds. Third, the heat required for calcination of limestone can be better used to melt more scrap.

The properties of lime as a flux in the BOF steelmaking operation play a significant role in controlling slag composition, which in turn results in producing good quality steels. Lime is also a major constituent of dolomite refractories which are used to line the steelmaking furnace. Because lime is in contact with gases, slag and metal over the various temperature and oxygen pressure ranges in the process operation, a study of the interactions between lime and the above process components is very important in understanding the behavior of lime in the BOF. Such an understanding is necessary not only to help prevent the lining of the BOF from deterioration, but also to provide the information needed for an understanding of the reactions between lime, slag and metal.

There are many problems associated with lime and its reactions with slags in the actual BOF refining process. As an example of a typical problem, when flux lime is added to the BOF slag, it competes with the lime of the vessel lining to bring the slag to saturation with lime. If the flux lime does not go into solution in the slag fast enough, then the lime from the lining will also take part in the slagging reaction, and the lining will deteriorate.

The dissolution of lime has been a topic of great interest to BOF steelmakers. A large number of investigations have been conducted to find the optimum properties of fluxing lime in relation to its rate and extent of solution. Although it is believed that the dissolution of lime in the slag occurs mainly through the interaction between lime and iron oxide, much work remains to be done on how the impurities in the slag and in the lime, influence its dissolution behavior.

The purpose of this work is to provide additional knowledge on the system lime-iron oxide. The work should be helpful both in establishing the effect of certain variables on the properties of lime and in better understanding the reaction mechanism whereby lime dissolves in the slag.

The objective of the present study was primarily to determine the solubility of iron oxide in solid lime at 1300° and 1400°C as a function of the partial pressure of oxygen. These experiments also involved measurements on the stability region of dicalcium ferrite from 1200° to 1438°C, with

respect to formation of liquid oxide and a lime-iron oxide solid solution. Results from the above experiments are presented as phase diagrams, and are discussed in terms of the behavior of lime in the BOF. Some experiments were also carried out on the rate of hydration of lime, lime-iron oxide solid solutions, and mixtures of lime-iron oxide solid solutions and other phases. Where possible, the hydration results are correlated with the phase equilibrium data obtained and with data from the literature.

II. REVIEW OF LITERATURE

As the present investigation involves three distinct types of experiments, a search of the literature is presented in the following order: A) The system CaO-iron oxide, B) Melting temperature of $2CaO \cdot Fe_2O_3$ with excess CaO as a function of oxygen pressure, C) Hydration tests on lime and mixtures of lime-iron oxides.

A. The System CaO-Iron Oxide

Studies on the system CaO-iron oxide have been reported by a great number of investigators. Several versions of this system have been published in the form of phase diagrams. The system CaO-iron oxide is not a true binary, because iron is present in different oxidation states, depending on the partial pressure of oxygen. However, the phase relations of the system have usually been expressed as pseudo-binary diagrams for the following two conditions: 1) The system CaO-iron oxide in equilibrium with metallic iron (i.e. under relatively reducing atmosphere); 2) The system CaO-iron oxide in air or at 1 atm oxygen pressure (i.e. under oxidizing atmosphere).

1. The System CaO-Iron Oxide in Equilibrium with Metallic Iron

A brief review of the earlier work related to this system was given by Cirilli and Burdese,[1] who investigated the phase relations of the system, and determined the mutual solid solubility of CaO and "FeO" by using X-ray and microscopic methods. The solubility limits of "FeO" in CaO varied

from 2.5%* "FeO" at room temperature to 11.3% "FeO" at the eutectic temperature, 1120°C, while those of CaO in "FeO" ranged from 0% CaO at 700°C to 7.6% CaO at 1120°C. Their study did not cover the solubility of "FeO" in CaO above the eutectic temperature. They also studied the reduction equilibrium of $2CaO \cdot Fe_2O_3$ in the presence of metallic Fe as a function of gas composition over the temperature range from 900° to 1050°C, and mentioned phase relations: Below 1070°C, phases of $2CaO \cdot Fe_2O_3$ and metallic Fe were in equilibrium. Above 1070°C, phases of CaO(ss), "FeO"(ss) and metallic Fe coexisted in equilibrium.

The phase equilibrium diagram determined by Allen and Snow[2] is given in Fig. 1, who also used the X-ray technique and microscopy. The features of this diagram are: The solubility limit of CaO in "FeO" is much larger than that of "FeO" in CaO. $2CaO \cdot Fe_2O_3$ is stable up to 1078°C, where it decomposes to CaO(ss), and "FeO"(ss); the latter phases coexist in equilibrium up to 1133°C. However, their values for the solubility of "FeO" in CaO are stated to be "estimated", based on X-ray data alone.

Tromel, Jager and Schurmann[3] established the phase diagram of the iron oxide-rich portion of the system CaO-"FeO". According to the diagram, $2CaO \cdot Fe_2O_3$ exists in stable equilibrium with metallic Fe up to 1160°C, where it melts

---

*% stands for weight percent throughout this thesis unless otherwise specified.

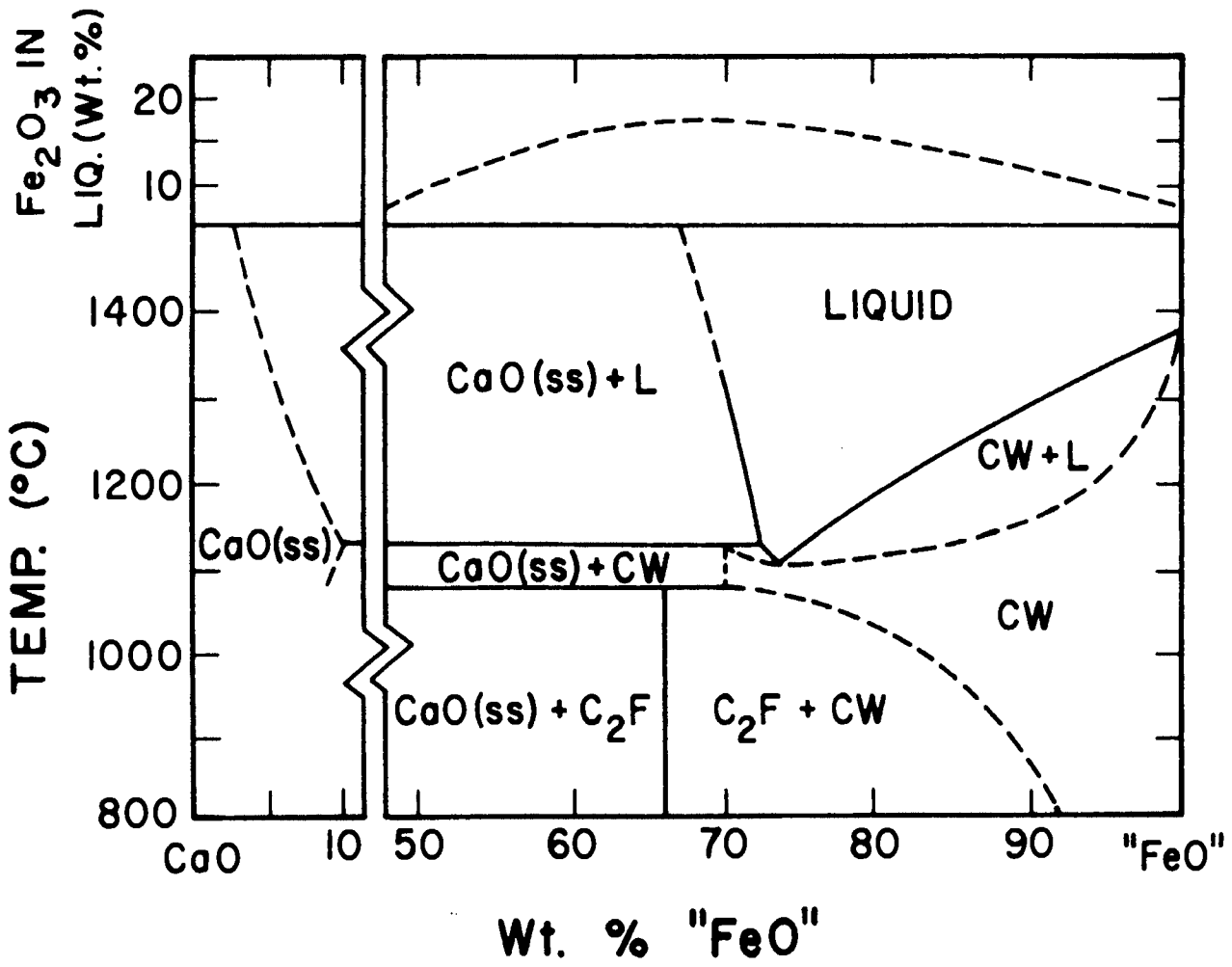

Figure 1. Phase Diagram for the System CaO-"FeO" in Equilibrium with Metallic Iron, after Allen and Snow.[2]

peritectically to CaO(ss) and liquid oxide. Comparing this with Fig. 1, a disagreement is noted with respect to the stability relations of $2CaO \cdot Fe_2O_3$.

Hahn[4] has thoroughly investigated the system CaO-"FeO" at 1090°C in the range of oxygen partial pressures from $10^{-13.444}$ to $10^{-14.540}$ atm. on the basis of X-ray data. His diagram is shown in Fig. 2. The features of his isothermal diagram relevant to the present work are as follows: The solubility limits of "FeO" in CaO and of CaO in "FeO" are considerably affected by the oxygen pressure. The maximum solubility of "FeO" in CaO is about $N_{"FeO"} = 0.12$ at $pO_2 = 10^{-13.725 \pm 0.31}$ atm., where $2CaO \cdot Fe_2O_3$ is in equilibrium with CaO(ss) and metallic Fe. He also determined an activity-composition curve for wustite in lime solid solutions at 1090°C.

A version of the phase diagram for CaO-"FeO" was published by Muan and Osborn,[5] and is shown in Fig. 3. The diagram is based mainly on the work of Allen and Snow,[2] but a reference to a study of Aukrust and Muan was given as an unpublished work. This diagram shows a much greater solubility limit of iron oxide in CaO than does Allen and Snow.[2]

Obst, Horn and Stradtmann[6] have extensively determined the solubility of iron oxide in CaO of the system CaO-"FeO" as a function of temperature. The solubility of iron oxide in lime decreases from 11.9% at 1160°C, the peritectic temperature, to 6.1% at 1700°C. They performed

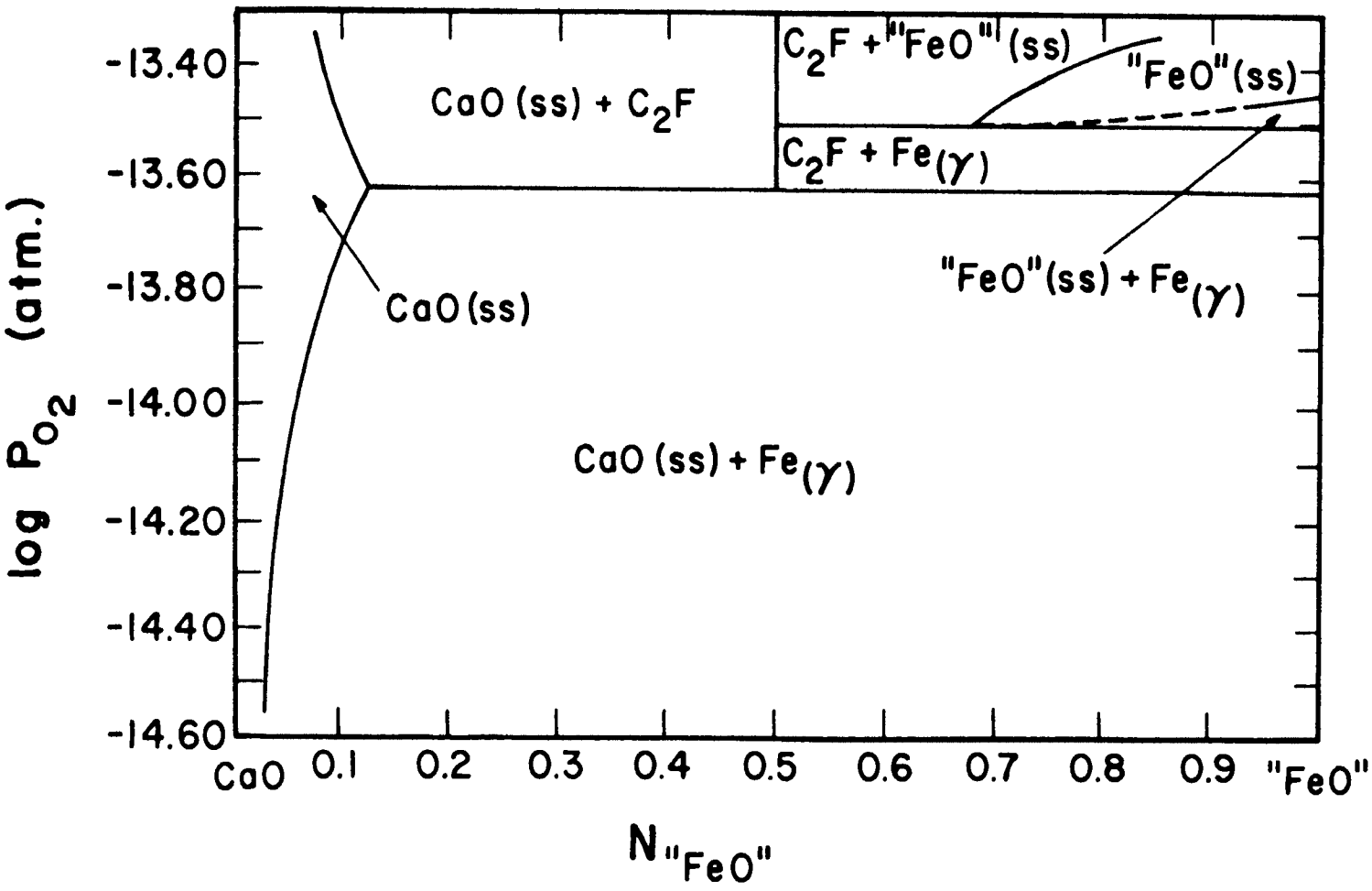

Figure 2. Phase Relations in the System CaO-"FeO" at 1090°C, after Hahn.[4]

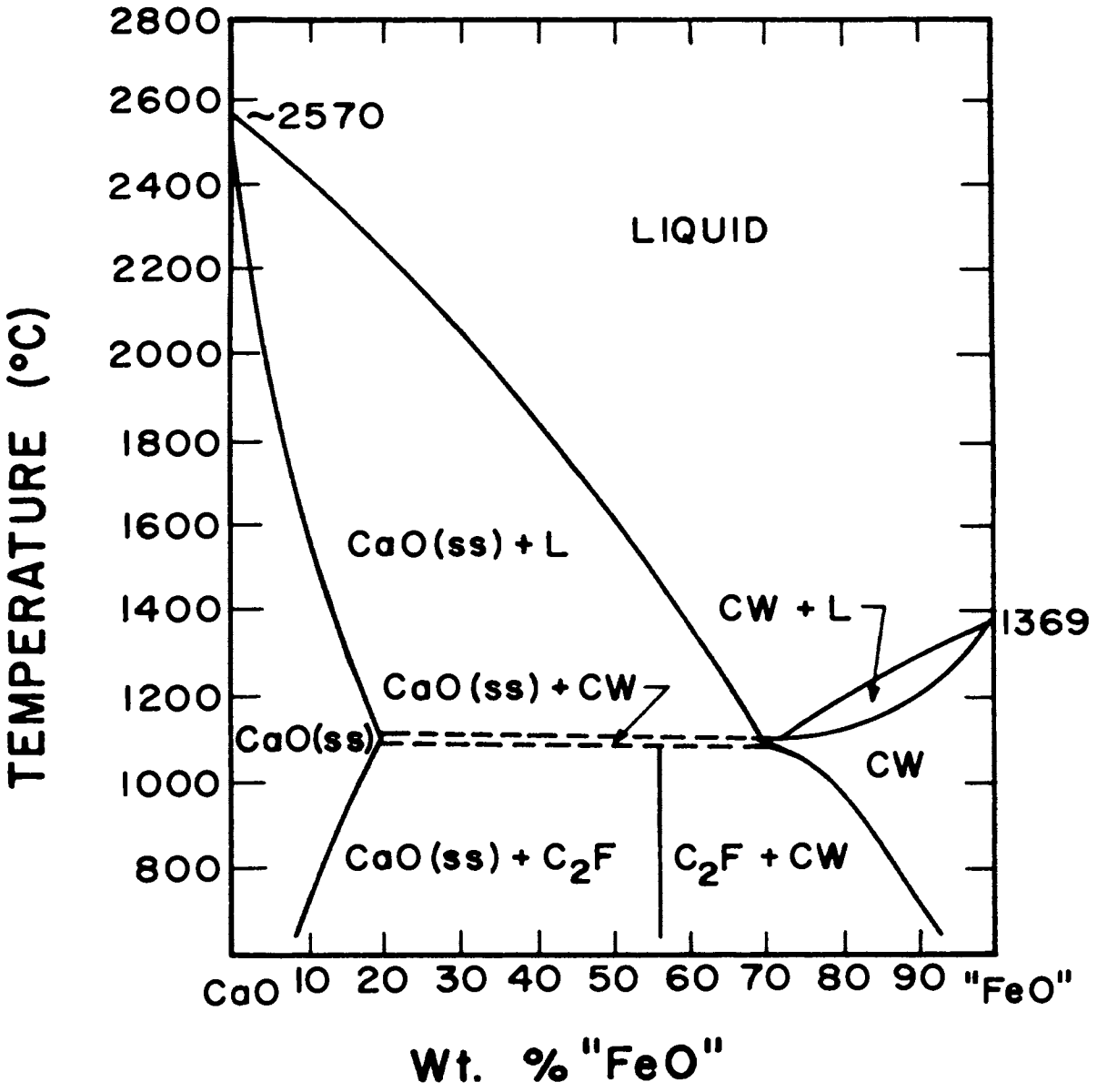

Figure 3. Phase Relations in the System CaO-Iron Oxide in Equilibrium with Metallic Iron, from Muan and Osborn.[5]

this work partly to illustrate the possibility of utilizing electron microprobe analysis for phase equilibrium studies. They conclude that this method can be used for the determination of both the phase boundaries (solidus and/or liquidus) and the location of tie lines. Their data show a little higher value for the solubility of "FeO" in CaO at 1300° and 1400°C than those of Allen and Snow.[2]

Fig. 4 is the most recent version of the system CaO-"FeO", established by Obst and Stradtmann.[7] They have collected the existing data and constructed the diagram based mainly on the works of Tromel et al.[3] and Obst et al.[6]

Besides studies on the phase relations there are several papers which deal with the thermodynamic properties of the system CaO-"FeO". Johnson and Muan[8] determined the activity of "FeO" in CaO(ss) at 1080°C. Fujita, Iritani and Maruhashi[9] determined activities of "FeO" and CaO in lime-iron oxide slags at 1650°C, using an MgO crucible and a rotating crucible furnace. Their values for the activity of "FeO" were discussed and compared with the published data of numerous other investigators. Koehler, Barany and Kelley [10] have compiled heats and free energies of formation of $2CaO \cdot Fe_2O_3$.

2. The System CaO-Iron Oxide under Oxidizing Conditions

Phillips and Muan[11] made a thorough review of the previously reported work on the system CaO-iron oxide at high oxygen pressures, and performed comprehensive investigations

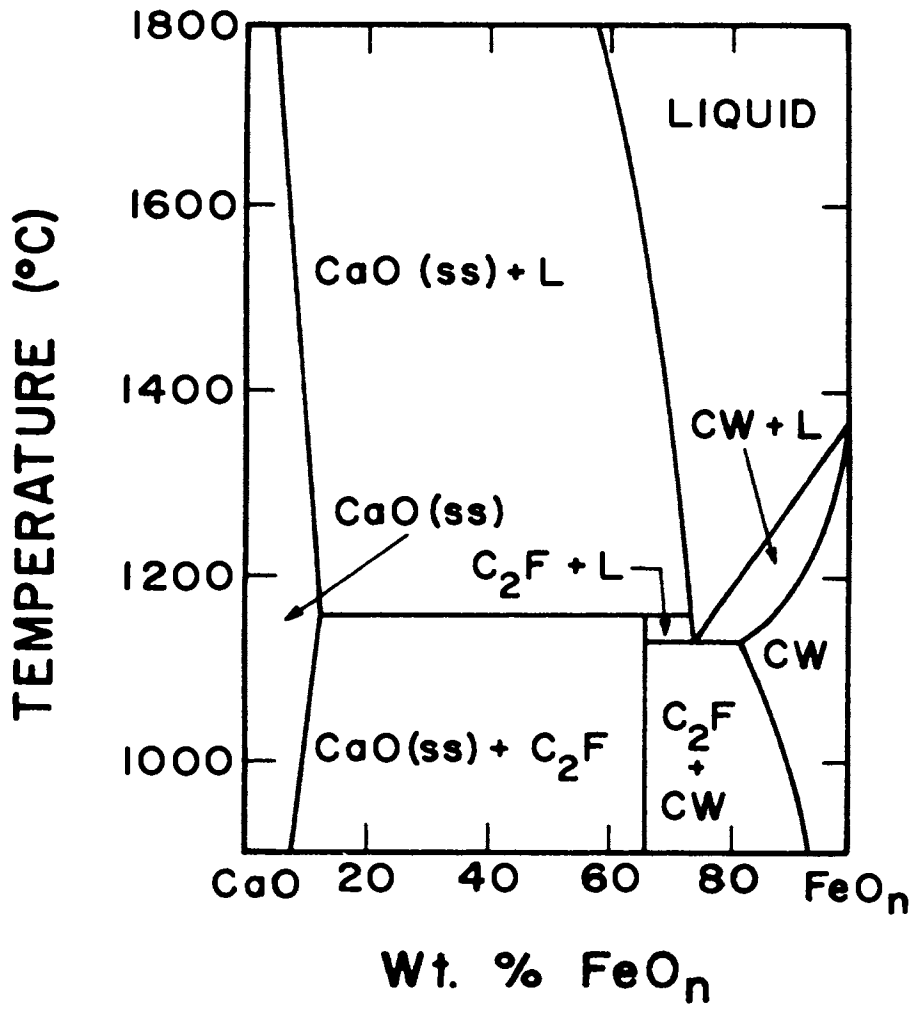

Figure 4. Phase Diagram for the System CaO-FeO_n in Equilibrium with Metallic Iron, after Obst and Stradtmann.[7]

on the phase relations of the system CaO-iron oxide in air and at 1 atm oxygen pressure. Their phase diagram of the system in air is given in Fig. 5. Some features of this diagram of interest to the present work are that there is no discernible solubility of Fe_2O_3 in solid lime, and stoichiometric $2CaO \cdot Fe_2O_3$ melts congruently at about 1450°C. The system CaO-iron oxide at 1 atm oxygen pressure is practically is the same as in air, except for CaO contents below about 21%. Phillips and Muan[12] have also delineated the phase relationships of the system $2CaO \cdot Fe_2O_3$-Fe_3O_4-Fe_2O_3 above 1135°C.

B. Melting Temperature of $2CaO \cdot Fe_2O_3$ with Excess CaO as a Function of Oxygen Pressure

A careful literature survey reveals that no systematic experimental studies have been performed on the measurement of the melting temperature of $2CaO \cdot Fe_2O_3$ in the presence of excess CaO as a function of oxygen pressure over a wide temperature range. The only melting or dissociation points of $2CaO \cdot Fe_2O_3$ that appear are in published phase diagrams, and have already been mentioned.

Among other available information, a study which is particularly related to the present work is that of Turkdogan.[13] He reviewed comprehensively the reported data in the literature. On the basis of these and from theoretical considerations, he has constructed an oxygen potential diagram for the system Fe-Ca-O. His Fig. 4 is shown in this work as Fig. 6. In his diagram, the univariant

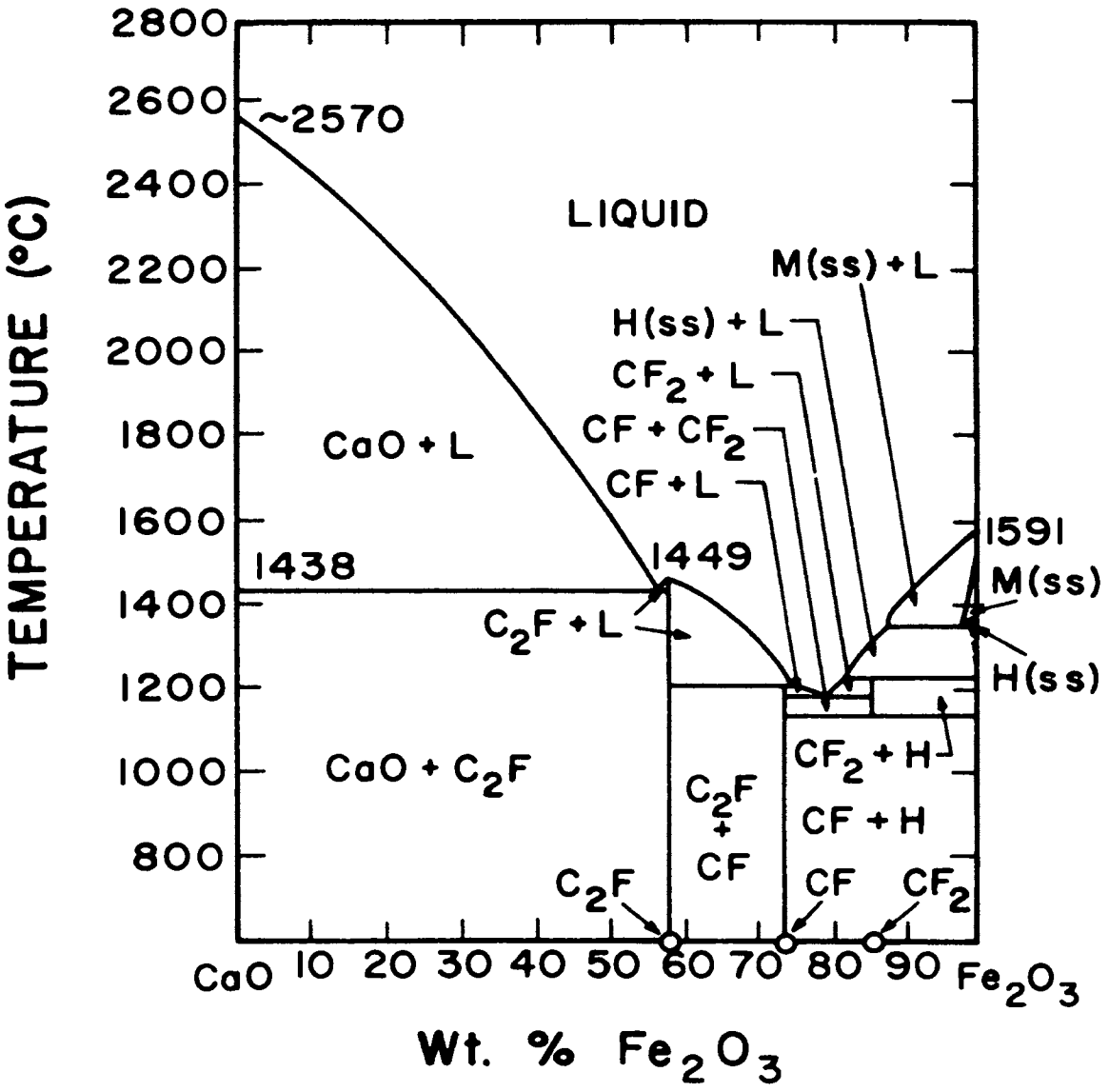

Figure 5. Phase Relations in the System CaO-Iron Oxide in Air, after Phillips and Muan.[11]

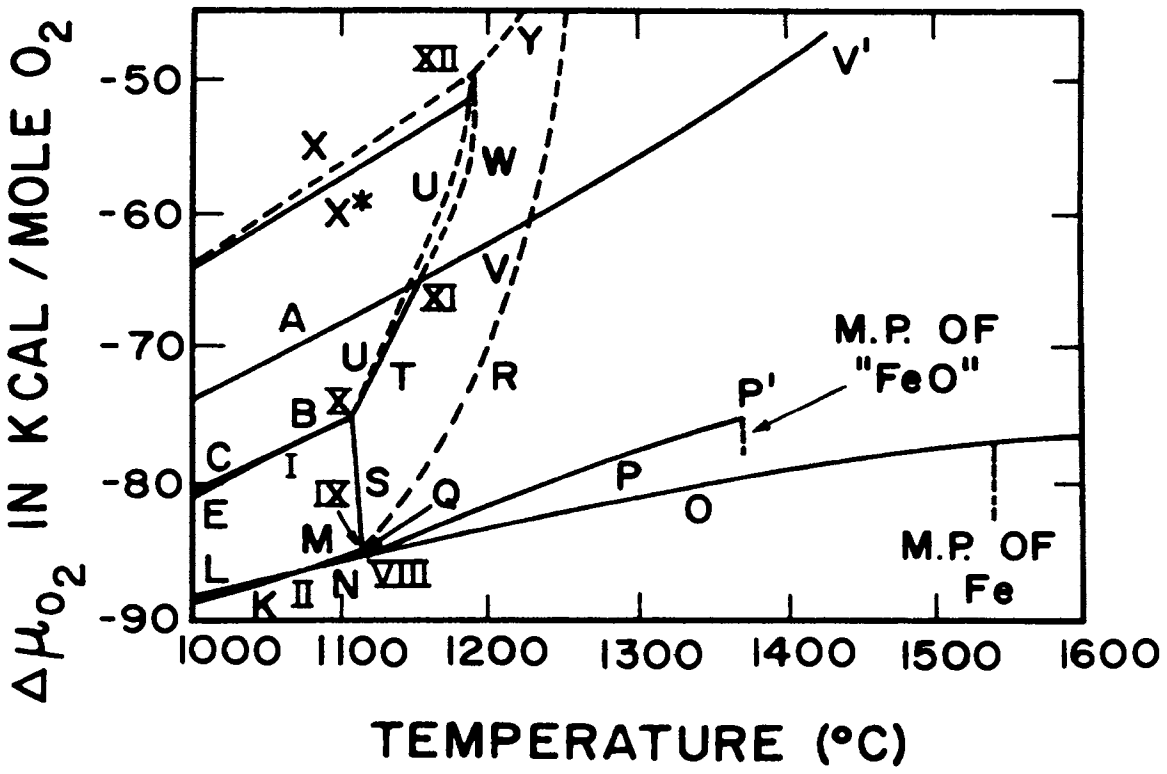

Figure 6. Oxygen Potentials of the Fe-Ca-O System in the Solid Plus Liquid State, after Turkdogan.[13]

O: Fe + CaO + MELT
P: Fe + "FeO" + MELT
Q: "FeO" + CaO + MELT
R: CaO + $2CaO \cdot Fe_2O_3$ + MELT
S: "FeO" + $2CaO \cdot Fe_2O_3$ + MELT
T: "FeO" + $CaO \cdot FeO \cdot Fe_2O_3$ + MELT
U: $2CaO \cdot Fe_2O_3$ + $CaO \cdot FeO \cdot Fe_2O_3$ + MELT
V: "FeO" + Fe_3O_4 + MELT
W: Fe_3O_4 + $CaO \cdot FeO \cdot Fe_2O_3$ + MELT
X: Fe_3O_4 + $CaO \cdot FeO \cdot Fe_2O_3$ + $2CaO \cdot Fe_2O_3$
X*: Above Equilibria, but from Reeve and Gregory[14]
Y: Fe_3O_4 + $2CaO \cdot Fe_2O_3$ + MELT

curve R is particularly relevant to this study, because it represents the stable coexistance of $2CaO \cdot Fe_2O_3$, CaO(ss), liquid and a gas phase.

Reeve and Gregory[14] experimentally checked a portion of Turkdogan's diagram over the temperature range 1000° to 1150°C. They found two discrepancies. One was the position of the invariant point X, which should be at an oxygen potential of -75.8 kcal/mole O_2 instead of Turkdogan's value of -75.1 kcal/mole O_2. The other was the slope of the univariant curve X. Their revised curve X* is shown in Fig. 6 as a solid line, just below the dashed line X of Turkdogan.[13] They also concluded that the curves R, U, W and Y which were proposed by Turkdogan also needed experimental verification. However, their work did not include measurement of the univariant reaction represented by curve R, which is of particular interest to the present work.

C. Hydration Tests on Lime and Mixtures of Lime-Iron Oxides

From the beginning of the use of lime as a flux in the BOF, attempts have been made to correlate the physical or chemical properties of lime with its performance in the BOF. Among the various properties of lime, the "reactivity" of lime has been considered to give a good indication of the dissolution rate of lime in the slag. In order to check the reactivity of lime, a water reactivity test such as the ASTM method[15] or the CGT method[16] is generally used by both lime producer and steelmaker. These methods measure the reactivity of lime toward water and classify the lime

into one of the following criteria; high reactive (soft burnt), medium reactive (medium burnt), or low reactive (hard burnt) lime.

Therefore, the water reactivity test has played an important role both for lime producer in correlating the reactivity of lime with the burning degree of lime and, in turn, for the steelmaker, lime reactivity with lime dissolution rate in the BOF slag. However, in the latter case, some controversy exists. Many published studies raise the question of whether any water reactivity test is suitable to predict the rate of lime dissolution in a BOF slag.

Several investigators have reported that the water reactivity test of lime resulted in consistency with the rate of lime solution; that is, the high reactive lime dissolved faster than low reactive lime in the slag. Other investigators report, however, that the reactivity with water is not consistent with the rate of lime dissolution. The following survey is a typical (but not exhaustive) account of the different reports on the subject.

Behrens, Koenizer and Kootz[17] used hard and soft burnt lime (classified by the CGT test) in actual BOF operations and concluded that soft burnt lime leads to a more rapid dephosphorization and better desulfurization, as well as an easier conduct of the heat with reduced slopping. Gregory et al.[18] used 3 different qualities of lime in a laboratory-scale experimental BOF and found that briquettes made from calcines of low water reactivity (by the ASTM and GLAC[18] methods) showed

a higher rate of slag formation. From this they pointed out that the water reactivity of lime is not necessarily a guide to the reactivity of lime in a slagmaking sense.

Limes[19] briefly introduced a crucible test which correlates the water reactivity of lime with the solution rate of lime in the slag. The crucible test is as follows: Samples of closely sized (-5+6 mesh) soft or hard burnt lime were mixed with synthetic slags in crucibles and inserted into a furnace at 2700°F and withdrawn at 2 minute intervals. A more detailed study on the above crucible test was presented by Russell,[20] who mentioned that the effective solution rate of lime can be determined by the ASTM water reactivity test and that soft burnt lime has a higher rate of solubility than hard burnt lime.

Konig, Rellermeyer and Obst[21] studied the results of the experimental BOF operations and of their laboratory experiments with iron crucibles containing various synthetic slags at about 1400°C, and concluded that the rate of lime dissolution is determined primarily by the following three factors; the formation of dicalcium silicate shells around the pieces of lime, the particle size of lime, and the composition and temperature of the slag. The small particles of the soft burnt lime react much more rapidly with the iron oxide than the large particles of the hard burnt lime. They also found that soft burnt lime dissolved 4 to 5 times faster in 90% FeO + 10% MnO slag than hard burnt lime. The solution rate for soft burnt vs. hard burnt lime was only about twice

as fast in iron silicate slags.

Based on the data obtained from actual BOF operations with soft, medium and hard burnt lime, Reinders, Friedl and Kauder[22] reported that the rate of lime dissolution in industrial BOF slags is higher for soft burnt lime than for hard burnt lime. Bardenheuer, Ende and Oberhauser[23] carried out dissolution experiments at 1600°C by immersing hard and soft burnt lime specimens in a ceramic crucible containing synthetic slag with similar composition to the initial BOF slag. They point out that no essential difference in the dissolution rate between hard and soft burnt lime is shown in slags with iron* contents below about 20%. With increased ferrous oxide contents, the dissolution rate of soft burnt lime is several times higher than that of hard burnt lime. Similar results were obtained by Bardenheuer, Ende and Speith.[24] They contended that when iron content in a BOF slag is less than about 20%, lime is surrounded by a dicalcium silicate layer. For these slags, the hard or soft burnt nature of the lime has no influence on the solution rate of the lime.

For iron contents over 20%, the surrounding dicalcium silicate layer is softer and the rate of solution of lime is much faster. No remarkable boundary structure in the

---

*The slag analyses in Ref. 23 and 24 are reported in terms of % iron. A slag containing 20% iron contains about 26% ferrous oxide.

slag, next to the lime particle, was observed. For slags containing over 20% iron the soft burnt lime dissolves much faster than hard burnt.

Leonard[25] reviewed thoroughly the work of Behrens et al.[17] and Gregory et al.,[18] and confirmed the results of Behrens et al.[17] on the basis of the plant trials with three 32-ton basic oxygen furnaces. He states that the water reactivity of lime is a major factor in determining the rate of slag formation. However, on account of the observed anomalous results, he also states: "The slaking methods of measuring reactivity are inadequate in that they do not ensure that reactive lime is recognized as such and presumably will be superseded by surface-area or density measurements."[25] Anderson and Vernon[26] illustrated the relationships between the water reactivity (ICI test)[26] and apparent density of lime, and between the water reactivity and moisture content absorbed by a low density lime. He pointed out that lime which has absorbed even a small amount of atmospheric moisture in handling and transit may be relatively inactive in the slaking tests though it will still dissolve in the slag at a rate consistent with its apparent density. They also studied the solution rate of lime in a synthetic slag at 1450°C by a modification of the crucible test developed by Republic Steel Corp.[19] The apparent density and particle size, and thus the external specific surface area of lime were found to be primary parameters affecting lime solution in a given slag.

Obst et al.[27] published a most extensive literature review and discussed extensively the effect of lime quality on the BOF steelmaking process. They explained the disagreement between the water reactivity test and the dissolution rate of lime in the slag to be caused by the reburning of soft burnt lime. Reburning is as bad for a quick dissolution of the lime as is the formation of a dicalcium silicate shell. They also described the use of prefluxed lime, composed of lime and fluxes such as pure iron oxides, $2CaO \cdot Fe_2O_3$, Al_2O_3, CaF_2 and borates. These additives reduce the melting point of $2CaO \cdot SiO_2$, and so by using such special lime, they showed it is possible to work against reburning and $2CaO \cdot SiO_2$-formation. Limes and Russell[28] confirmed again the correlation between the water reactivity of lime and the rate of lime dissolution in slag based on the crucible test, but also mentioned that the crucible test has been used for screening and evaluation of prereacted products which would reduce the water reactivity values.

Schlitt and Healy[29] made a detailed comparison between the ASTM slaking rate test and German CGT test by using three types of lime (soft, medium and hard burnt). They developed a new water reactivity test (Scaled-Down Titration test) based on the German test. They pointed out the suitabilities of the ASTM and CGT tests for determination of the degree of lime burning, and of the SDT method for testing lime produced under closely controlled conditions.

Obst and Stradtmann[30] explain the desirability of

designing a new test method which is capable of predicting the rate of dissolution of lime in the slag. However, as yet, no such new test has been reported in the literature.

There are also a number of investigations which deal more with the interaction between lime and slag rather than with the water reactivity of lime. Pehlke and Klaas[31] carried out a kinetic study on lime solution in basic slags over a temperature range from 1400° to 1470°C. They immersed prepared lime cylinders in various synthetic slags contained in iron and other crucibles under argon atmosphere. After a given period of time, the crucibles were removed and quenched in an argon blast. The samples were examined by the optical microscope, and analyzed by the electron microprobe. From their results, they conclude that the solution of lime in basic slags is controlled by diffusion of iron [oxide] into the lime particle, and, to some extent, by the diffusion of calcium out of the lime particle.

Leonard[32] also conducted a kinetic study on the dissolution of CaO over the temperature range 1250° to 1450°C by immersing CaO cylinders (single crystals and ceramic specimens) in iron crucibles containing iron oxide-CaO liquids under an argon atmosphere. Based on electron microprobe analyses, he concluded that in his samples, Fe^{++} does not diffuse into the single crystal during the corrosion process, therefore the mass transfer process is one of dissolution and not solute gradient melting. In the presence of free convection currents, diffusion of reactant into the solid to form

the liquidus composition at that temperature is not a necessary condition for mass transfer. His observations differ from others[7,31,33,34] who used a different type of lime.

Schlitt[33] performed a study on the dissolution of lime in calcium-iron silicate slags at 1375°C by using an immersion method. He concluded that the rate of lime dissolution was dependent on the composition of the slag, but not on the type of lime or the reaction time. Dissolution occured by diffusion of iron [oxide] into the solid lime and penetration of a calcium-iron oxide liquid phase into the pores. Lime dissolved into the liquid and then diffused out into the slag. He reviewed several investigations which dealt with the mechanism of lime solution in the slag.

Obst, Stradtmann and Horn[34] and Obst and Stradtmann[7] contacted crystalline lime with liquid iron oxide in an iron crucible at 1400°C for 3 to 10 seconds and then quenched into water. The samples were examined by the optical microscope, and analyzed by the electron microprobe. From their data, they conclude that the dissolution of lime into the iron oxide melt involves the formation of a lime-iron oxide solid solution. Derge and Shegog[35] observed the dissolution mechanism of lime in synthetic slags of CaO-SiO_2 by using a hot filament microscope and explained that the solution of CaO and other basic oxides in highly basic slags is inhibited by the formation of a glass-like film which is highly protective. The change of volume associated with the crystallization of this film leads to spalling and more rapid solution.

Apparently, no crucible or water reactivity test is yet entirely satisfactory in predicting the dissolution rate of different limes in an operating BOF. Crucible tests seem to be inherently more suited to the task, but these tests do not reproduce such BOF conditions as continuously increasing temperature, turbulence, and changing slag composition.

III. EXPERIMENTAL METHOD

A. Furnace and Temperature Control

Samples were equilibrated in a vertical tube furnace heated by silicon carbide resistance elements. Three mullite tubes, 5/8 in I.D. and 40 in long, were in the furnace. A small side arm for gas introduction was attached to the end portion of each tube so that gases admitted could flow upward in each tube. The bottom of the tube was sealed by a rubber stopper which could be removed when quenching the samples, without disturbing the gas flow. The top of the tube was also sealed by a rubber stopper having a small ceramic tube through its center. The small ceramic tube had dual role of serving as gas outlet and as a supporter for the sample holder. A sketch of the furnace tube is shown in Fig. 7.

The temperature of the furnace was controlled by a millivolt pyrometer, with an accuracy of ±2°C. The control thermocouple was of Pt/Pt-13% Rh, inserted near the hot zone of the furnace. Measurements of the sample temperature were performed right before and after each equilibration run with three Pt/Pt-10% Rh thermocouples inserted into each of the mullite tubes. These thermocouples were calibrated periodically against a reference thermocouple of the same material that was standardized by the National Bureau of Standards at 1200°, 1300° and 1400°C. The thermal gradient of the furnace at the hot zone did not exceed 0.5°C over one inch.

B. Control of Atmosphere

The oxygen pressures in the controlled atmosphere of the

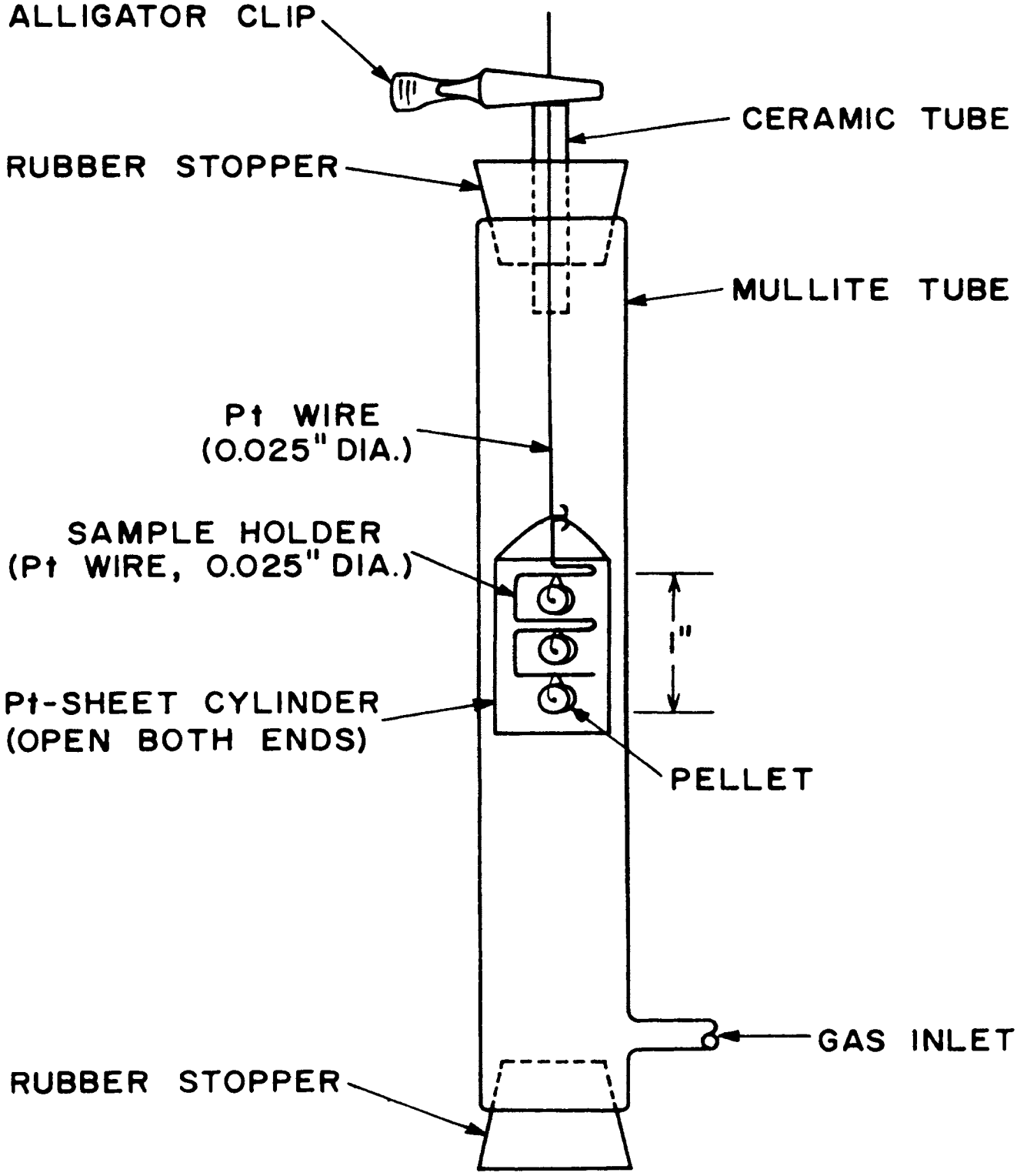

Figure 7. A Sketch of the Furnace Tube and Sample Arrangement. Three Tubes Similar to the Above Were in the Furnace at Once.

furnace ranged from 0.21 atm to about 10^{-14} atm. A wide range of desired oxygen partial pressures was obtained by mixing gases such as CO_2 (Coleman Instrument grade, reported purity 99.99% min. by vol.), CO (C.P. grade, 99.5% min.) and by use of various premixed cylinders of CO_2-CO, O_2-N_2, and O_2-Ar. All gases were supplied and analysed by Matheson Gas Products. Except pO_2 = 0.21 atm which is air, the oxygen partial pressures from $10^{-1.00}$ to $10^{-4.00}$ atm were produced by using either pure CO_2 or premixtures of O_2-N_2 and O_2-Ar. Oxygen partial pressures lower than $10^{-4.00}$ atm were generated by any of the following methods: 1) mixing CO_2 and CO from separate cylinders in the proper ratio, 2) flowing a premixed gas with a fixed CO_2/CO ratio, 3) mixing the appropriate amounts of two premixed gases with different CO_2/CO ratios, 4) changing the CO_2/CO ratio of a premixed gas by adding CO_2 or CO. The partial pressure of oxygen at the experimental temperature was calculated from tables of thermodynamic properties.[36]

The method of mixing was principally the same as that used by Darken and Gurry[37] and later by Johnson and Muan[8] and Timucin.[38] In particular, gas mixtures of known composition were obtained at room temperature after passing other gases individually through the calibrated flowmeter tubes of a Model 665 Matheson Gas Proportioner. Each flowmeter tube was repeatedly calibrated with a soap bubble column. This column consisted of a glass buret of known volume with a small reservoir of soap solution at the bottom.

The flow rate of gas through the flowmeter tube could be calculated by measuring the time for the ascension of a thin soap bubble. A soap solution saturated with CO_2 was used for the calibration of CO_2 and premixed gases containing CO_2 because of the relatively high solubility of CO_2 in water.[39] For the calibration of other gases, a solution was used without CO_2 saturation.

A gas flow rate of 110 cm^3/min was maintained in each tube to prevent the effect of thermal diffusion.[37]

C. Preparation of Starting Materials

1. Pellets

The source of CaO was Mallinckrodt analytical reagent grade, primary standard $CaCO_3$ with a label analysis given in Appendix A. About 5 gm of $CaCO_3$ was loosely filled into a Pt crucible and heated at 400°C for 24 hours in air. As no weight loss was shown, $CaCO_3$ was subsequently used without any preliminary treatment.

Fisher certified reagent grade Fe_2O_3 (analysis in Appendix A) was used for iron oxide. The loss on ignition of Fe_2O_3 was found to be 0.5% by heating about 20 gm in a Pt crucible at 800°C for 24 hours in air. Therefore all Fe_2O_3 was ignited and ground to -100 mesh prior to its use.

To make about 10 gm of a desired final composition of CaO-"FeO", proper amounts of $CaCO_3$ and Fe_2O_3 with the gravimetric factors of 1.765 and 1.111, respectively, were weighed out and mixed. The mixing and grinding were carried out in a porcelain mortar and pestle under reagent grade

acetone to ensure better mixing. This was continued until the sample was dried (about half an hour) and was repeated at least twice for complete mixing. The mixed powders were placed into a smooth alumina crucible and slowly heated in air up to 1000°C, and kept for 24 hours at 1000°C for calcination and sintering. The sintered mixture formed a loose pellet. The pellet was removed from the crucible and then was ground to -200 mesh in an alumina mortar and pestle.

A number of disc-shape pellets were made from this powder with a specially designed tool steel die. Each pellet, 7 mm in diameter and 2 mm in thickeness, had a small hole through the center and weighed approximately 200 mg. A certain amount of butyl alcohol was added to the powder as a binder during pelletizing. The pellets were sintered in air at 1300°C for one hour and then stored in a desiccator.

Sample pellets were prepared to have a series of compositions from about 0.5 to 12.0% "FeO" at intervals of about 0.5 weight % in "FeO" content. These pellets served as starting materials for all equilibration runs.

2. Powdered Sample ($2CaO \cdot Fe_2O_3 + CaO$)

A total weight of about 10 gm of powdered sample having a composition of 50% CaO-50% Fe_2O_3 was made by the following procedure: a) mixing proper amounts of $CaCO_3$ and Fe_2O_3 by the same steps as above, b) pressing the mixture into a 1 inch diameter pellet, about ½ inch thick, c) slowly heating the pellet in air in a Pt crucible up to almost 1440°C (slightly lower than the solidus temperature of this mixture

in air)[11] and holding it for 8 hours, d) air cooling the sample out of the furnace, and e) grinding the resulting sample to -100 mesh. The powder was also stored in a desiccator.

D. Equilibration Runs

1. Pellets

3 pellets with different bulk compositions were suspended by a thin Pt-wire sample holder (which was designed to minimize pickup of iron from the sample), and then lowered into the hot zone of a furnace tube (see Fig. 7) at the chosen temperature. The bottom of the tube was sealed tightly by a rubber stopper, and a high flow rate of gas was admitted through the side inlet attached to the furnace tube. After the air was flushed out, the flow rate was reduced to about 110 cm^3/min.

In order to determine the time required to reach equilibrium, a number of pellets with a fixed composition were held at a given temperature and low oxygen partial pressure for various time intervals, and then were quenched. Examining these samples under a metallograph, it was found that no further phase changes were observed in the samples after 12 and 72 hours at 1400° and 1300°C, respectively. Samples in actual runs were maintained for 24 hours at 1400°C, and 72 hours to a week at 1300°C. After equilibration, the samples were quenched into isopropyl alcohol at room temperature by releasing the sample holder at the top of the tube. The furnace temperature and atmosphere were not disturbed by this

quenching technique. Throughout this experiment isopropyl alcohol was always used as a quenching medium instead of water, because of the high CaO content in the sample.

2. Powdered Sample ($2CaO \cdot Fe_2O_3$ + CaO)

About 200 mg of the powdered sample (with the composition of 50% CaO-50% Fe_2O_3) was put into a small Pt envelope and suspended in the hot zone of the tube at a selected temperature and oxygen pressure. After holding 4 to 6 hours the crucible was quickly pulled to the top of the tube and cooled.

E. Phase Identification

The quenched samples were dried, removed from the sample holder, divided into smaller pieces, and mounted in Koldmount (self-curing resin) for subsequent examination. The mounted sample was prepared for microscopic examination by first grinding it on a series of carborundum papers with decreasing grit sizes, and then polishing it on a cloth wheel with "Linde C" alumina abrasive suspended in methanol.

Microscopic examinations were conducted to identify the phases present in the sample. Actual phase determinations were carried out on the metallograph at various magnifications from 100 to 500X, using bright field, sensitive tint and polarized light. The quenched liquid phase was clearly distinguished from the other solid phases; in small amount, it had a sharp-edged shape and appeared usually at the grain boundaries of the lime solid solution matrix, and was colored dark brown under polarized light. The typical shape and the coloration were advantageous in recognition of a trace amount

of the liquid phase present. Dicalcium ferrite showed as comparatively large round spots, and was readily recognized under polarized light by its dark brown color. Metallic iron appeared as very small shiny specks in the bright field. It turned to deep purple in the sensitive tint and was black under the polarized light. Most samples were not etched, but to confirm the presence of very small amount of liquid or metallic iron, some samples were etched by water or by dilute HCl (about 1% HCl). Although the change in color was greatly helpful in distinguishing metallic iron, the greatest difficulty occured in identifying a trace amount of metallic iron, because some of the polished samples had picked up small amount of impurities from carborundum papers during the first stage of polishing, and these impurities looked like metallic iron in the metallograph.

The samples used to find the melting temperature of dicalcium ferrite were not examined microscopically, since visual examination was sufficient to tell whether the sample had melted or not.

F. Chemical Analysis

Chemical analyses were carried out to determine the compositions of all the prepared starting pellets. The method of chemical analysis was essentially similar to that used by Timucin[38], and is described briefly in Appendix B.

G. Hydration Tests on Lime and Mixtures of Lime-Iron Oxides

In addition to the quenching experiments for the determination of solubility of iron oxide in lime, some hydration

experiments were conducted to examine the stability of lime-iron oxide mixtures and solutions toward moisture, as compared to the stability of pure lime.

The starting material for the pure lime pellet was CaO, which was obtained by calcining pure $CaCO_3$ in a Pt crucible at 1300°C for 24 hours. For the pellets containing various amounts of iron oxide, the lime mentioned above and the Fe_2O_3 previously prepared were used. The method of pelletizing was similar to that described earlier. The details of pellet sintering conditions prior to the hydration runs are presented in Table I.

In Table I, the phases present during sintering of the pellets are also listed. For the pellets sintered at 1200°C, the information on phases present was obtained from experimental data taken from early stages of equilibration runs. For the pellets sintered at 1400° and 1450°C, the phases present were deduced from Fig. 5. The phases in some of the samples were also confirmed by microscopic examination of quenched pellets.

The amount of $2CaO \cdot Fe_2O_3$ present in the samples sintered at 1400°C increased with increasing Fe_2O_3 content. The pellets sintered at 1450°C consisted of CaO and liquid at equilibrium, but after cooling they also had a small amount of $2CaO \cdot Fe_2O_3$, and perhaps other calcium ferrites. The presence of $2CaO \cdot Fe_2O_3$ was due to the decomposition of all or a part of the liquid phase during cooling, depending on the rate of cooling. The amounts of liquid phases of the last

Table I Details of Pellet Sintering

Sample Number	Pellet Composition	Sintering Temperature	Sintering Condition	Phases Present During Sintering
S1-1	Pure CaO		Pellets were held at $pO_2=10^{-11.8*}$, for 30 hours, pulled to top of furnace.	CaO
S1-2	CaO - 1½% "FeO"		Pellets were equilibrated	CaO(ss)
S1-3	" - 4% "	1200°C	in Pt crucible at $pO_2=10^{-11.8*}$	CaO(ss)
S1-4	" - 8% "		for 30 hours, and then quenched	CaO(ss)+Liq.(tr)
S1-5	" - 12% "		into alcohol.	CaO(ss)+Liq.(m)
S2-1	Pure CaO		Pellets were sintered in Pt	CaO
S2-2	CaO - 1½% Fe_2O_3		crucible in air for 6 hours,	$CaO+C_2F$
S2-3	" - 4½% "	1400°C	and then cooled in air outside	$CaO+C_2F$
S2-4	" - 9% "		the furnace.	$CaO+C_2F$
S2-5	" - 13% "			$CaO+C_2F$
S3-1	CaO - 1½% Fe_2O_3		Sintering and cooling method was	CaO+Liq.
S3-2	" - 4½% "	1450°C	the same as above except for	CaO+Liq.
S3-3	" - 9% "		temperature difference.	CaO+Liq.
S3-4	" - 13% "			CaO+Liq.

(Table I continued)

Sample Number	Pellet Composition	Sintering Temperature	Sintering Condition	Phases Present During Sintering
S4-1	CaO - 1½% Fe_2O_3		Sintering of pellets was exactly	CaO+Liq.
S4-2	" - 4½% "	1450°C	the same as above except that	CaO+Liq.
S4-3	" - 9% "		samples were quenched into	CaO+Liq.
S4-4	" - 13% "		alcohol.	CaO+Liq.

*It is believed that the actual oxygen partial pressure generated in the furnace tube(1½ in I.D.) in which the samples were equilibrated at 1200°C was somewhat lower than $pO_2=10^{-11.8}$ atm, because it was found later that thermal diffusion in the larger tube affected the calculated pO_2.

two sets of samples, S3 and S4, were proportional to the Fe_2O_3 content.

After sintering, each pellet weighed approximately 1 gm and had a cylindrical shape. The diameter was ¼ in, and the average height ½ in.

In order to conduct the hydration test under a controlled moist atmosphere, it was necessary to have an aqueous solution which could provide constant humidity in an enclosed space at room temperature. For this purpose a solution was prepared that was saturated with potassium carbonate. This solution maintained a relative humidity of 42.8% at 25°C.[40]

Each of the prepared pellets was initially weighed in a small tared container. After weighing, all pellets were placed in the humidity chamber, over the K_2CO_3 solution. The weight gains of these pellets were checked at appropriate time intervals. During the weighing procedure, all samples were taken out of and put back into the humidifier at the same time so that they were exposed for an equal period of time to room air and to the moist atmosphere.

IV. EXPERIMENTAL RESULTS AND DISCUSSION

The present investigation consisted of three distinct types of experiments as described earlier. The results of the experiments and their discussion will be presented in the following order: 1) Measurement of the melting temperature of dicalcium ferrite in the presence of excess lime; 2) Determination of the solubility limits of iron oxide in solid lime; 3) Hydration tests on lime and mixtures of lime-iron oxides.

A. Presentation of Results

1. Measurement of the Melting Temperature of Dicalcium Ferrite in the Presence of Excess Lime

According to the published phase diagrams for the system CaO-iron oxide, dicalcium ferrite probably melts incongruently at low pO_2, and congruently at high pO_2. Thus the presence of excess CaO has no effect on the melting point of dicalcium ferrite at low pO_2, but does have a small effect at high pO_2. As explained earlier, all samples used for this part of the work contained excess CaO, so that the term "melting point" is not entirely correct for measurements made at high pO_2. Since the difference is small, and occurs only at high pO_2, the term "melting" was chosen to describe the equilibrium temperature between dicalcium ferrite, CaO(ss), liquid, and gas. This "melting" temperature is the same as the solidus temperature in the high-lime end of the system.

A graph of the experimental data for the determination of the melting temperature of $2CaO \cdot Fe_2O_3$ in the presence of

excess CaO is shown in Fig. 8. The experimental data taken in the investigation, and used to plot Fig. 8, are presented in Table II of Appendix C.

In the diagram, solid and open circles show if a liquid phase was absent or present during each experiment. The melting curve of $2CaO \cdot Fe_2O_3$ as a function of log pO_2 was drawn through the data points with a French curve. Above the curve, $2CaO \cdot Fe_2O_3$ and CaO(ss) exist as stable solid phases. Below the curve, the stable phases are liquid oxide and CaO(ss). The data obtained on the pO_2 for melting $2CaO \cdot Fe_2O_3$ at 1300° and 1400°C (from Fig. 8), were used in the construction of Figs. 9 and 10, presented later.

A notable feature of the diagram is that the melting curve shows a nearly linear dependence between the log of the oxygen pressure and 1/T°K (melting), up to about 1400°C, and then shows a sharp increase up to 1438°C. In other words, oxygen pressures above about 1 atm have little effect on the melting temperature of $2CaO \cdot Fe_2O_3$.

2. Determination of the Solubility Limits of Iron Oxide in Solid Lime

The results of the pellet quenching experiments at 1300° and 1400°C are plotted in Figs. 9 and 10, respectively, as a sort of phase diagram for the system CaO-"FeO". In the diagrams, the phase relations are shown as a function of oxygen partial pressure, and composition. The range of oxygen partial pressures investigated was from $10^{-8.00}$ to $10^{-12.16}$ atm at 1300°C (Fig. 9) and from $10^{-6.56}$ to $10^{-11.50}$ atm at

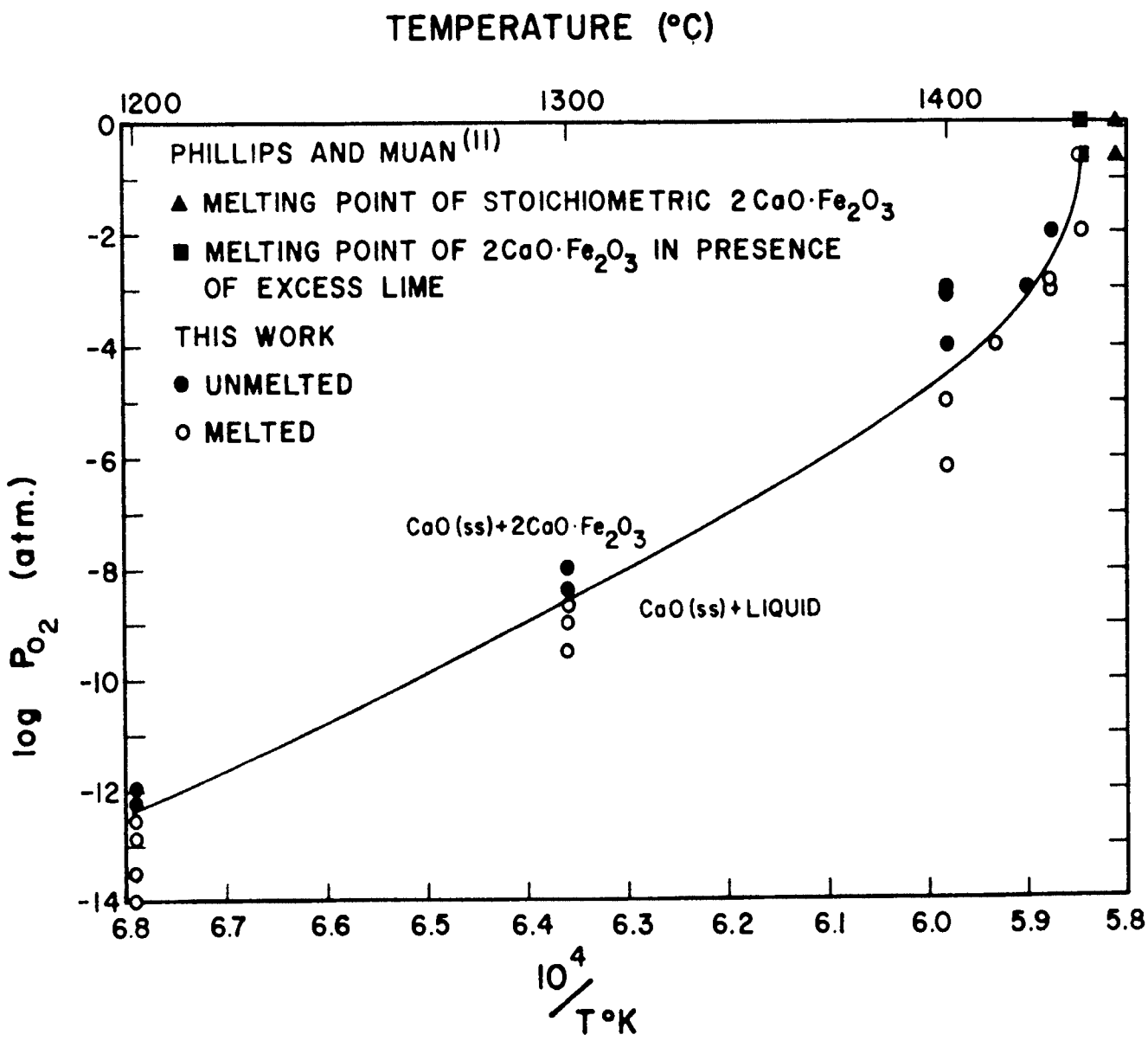

Figure 8. Melting Temperature of Dicalcium Ferrite in the Presence of Excess Lime.

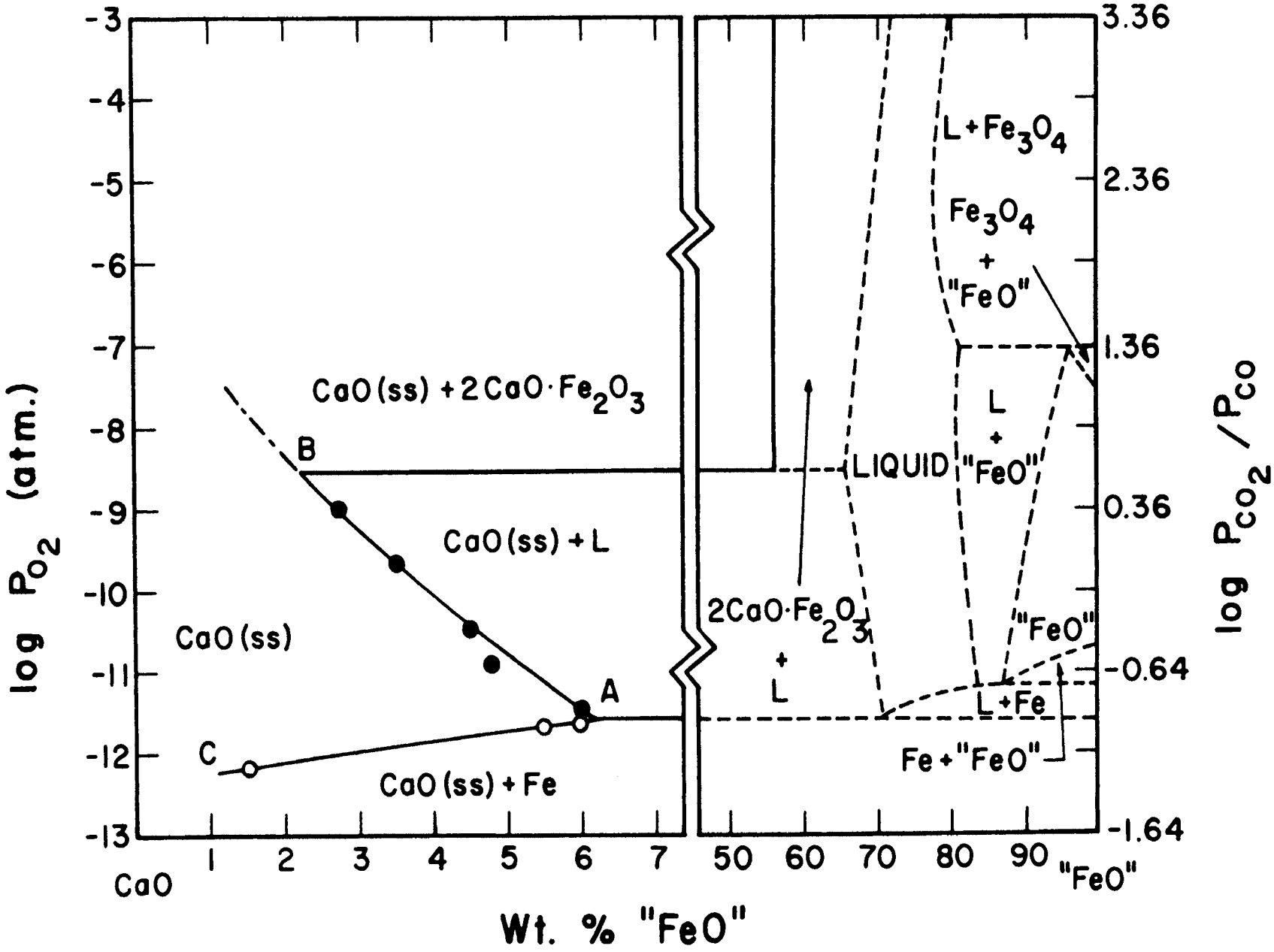

Figure 9. Solubility of Iron Oxide in Solid Lime at 1300°C.

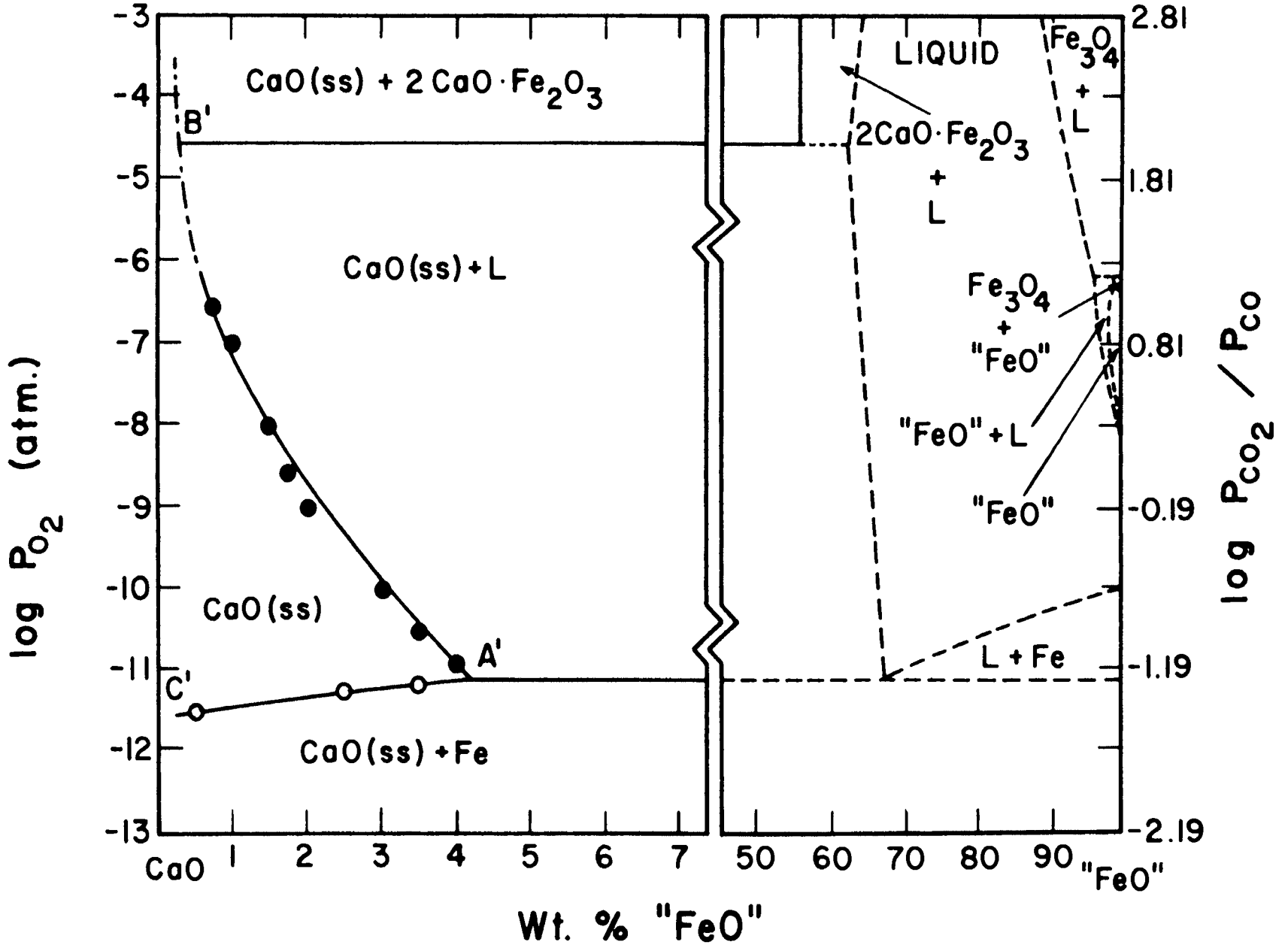

Figure 10. Solubility of Iron Oxide in Solid Lime at 1400°C.

1400°C (Fig. 10). Knowledge about the limits of the $2CaO \cdot Fe_2O_3$ stability region was based on the data obtained in $2CaO \cdot Fe_2O_3$ melting temperature experiments (Fig. 8), as mentioned earlier. The experimental data used for constructing these diagrams are summarized in Tables III and IV of Appendix C.

In each of the diagrams, solid and open circles represent the chemical compositions of CaO(ss) in equilibrium with liquid oxide and with metallic iron, respectively. To express the compositions as the chosen components of CaO and "FeO", the term iron oxide or "FeO" is used. This means that the actual amounts of Fe^{++} and Fe^{+++} present in the sample were not separately determined, but the sample was analysed for total iron and this amount was converted to hypothetical stoichiometric FeO. The points drawn on the diagrams are representative positions of the boundary curve drawn from the data of several runs at different compositions at fixed pO_2. This aspect of diagram construction is discussed in detail in Appendix C, where the data are presented.

The solid curve (AB in Fig. 9 and A'B' in Fig. 10) passing through the solid circles is the boundary line that separates the single phase region of CaO(ss) from the two phase region of CaO(ss) + liquid oxide. This curve represents a univariant equilibrium situation; CaO(ss) and liquid are in equilibrium with a gas. The solid curve (AC in Fig. 9 and A'C' in Fig. 10) passing through the open circles is the phase boundary between the fields CaO(ss) and CaO(ss) +

metallic Fe. This curve also represents a univariant equilibrium situation; CaO(ss) and metallic Fe are in equilibrium with a gas. As mentioned earlier, the exact position of this boundary was difficult to determine. Part of the difficulty was that the metallic Fe present in the sample was difficult to distinguish from the impurities picked up from carborundum papers during fine grinding. The electron microprobe was not very helpful in identifying iron because most of the particles appearing in the samples were too small to be accurately identified by this method.

The maximum solubility of iron oxide in CaO (point A in Fig. 9 and A' in Fig. 10) was determined by the intersection of the two solid curves (AB and AC in Fig. 9 and A'B' and A'C' in Fig. 10), and found to be approximately 6.2% "FeO" at 1300°C and 4.2% "FeO" at 1400°C. The oxygen partial pressure thus obtained is approximately $10^{-11.60}$ and $10^{-11.10}$ atm, respectively. At each of these particular oxygen pressures, an invariant equilibrium situation occurs; CaO(ss), liquid and metallic Fe coexist in equilibrium with a gaseous phase.

The points B in Fig. 9 and B' in Fig. 10 are determined by the intersection of the extended boundary line separating CaO(ss) from CaO(ss) + liquid, and the oxygen isobar at which $2CaO \cdot Fe_2O_3$ melts incongruently. At this oxygen pressure an invariant equilibrium situation also exists; CaO(ss), $2CaO \cdot Fe_2O_3$ and liquid are in equilibrium with a gas.

The dash-dot curve in each of the diagrams (in the vicinity of points B and B') is an inferred phase boundary [4,5,11] distinguishing the CaO(ss) region from the two phase areas. Although the primary objective of the present investigation is to establish the solubility limit of iron oxide in solid lime over a large range of oxygen pressures, the above boundary was not experimentally determined in the present work. Equilibrium between CaO(ss) containing very small amounts of "FeO" and these phases was found to take an extremely long time, and may not have been attained in even the longest runs made (7 days).

The exact phase relationships in the iron oxide-rich portion of the system (expressed as dashed lines) are unknown. No measurements in this part of the system were made, since it was beyond the scope of the present investigation. However, possible phase boundaries are included in Figs. 9 and 10 for the purposes of orientation. These boundaries are consistent with known data in the iron-oxygen system, and with the small amount of data available from earlier work.[4,5,11,37,41]

Some important features of these isothermal phase diagrams are as follows:

1) Two invariant equilibrium situations occur at both temperatures, where lime is a stable phase. These situations correspond to the upper and lower limits of an area at which CaO(ss) and liquid coexist in equilibrium.

2) Within the range of the upper and lower limits,

the solubility of iron oxide in CaO increases as the oxygen partial pressure decreases.

3) When metallic Fe is present, a very small decrease in oxygen pressure results in a substantial decrease in solid solubility of iron oxide in CaO.

3. Hydration Tests on Lime and Mixtures of Lime-Iron Oxides

The results of the weight gains of samples are graphically presented in Figs. 11(a) through 11(d) according to the pellet sintering condition (see Table I). The data for pure lime used in plotting Fig. 11(b) are reused in plotting Figs. 11(c) and 11(d) to compare pure lime with samples containing Fe_2O_3. The actual data used for plotting these curves are listed in Table V of Appendix C.

In Table V the increase in sample weight is expressed in terms of % $Ca(OH)_2$ formed according to the following hydration reaction:

$$CaO + H_2O \rightarrow Ca(OH)_2 \qquad (1)$$

The calculations were made on the basis that the lime in the sample proceeds to complete hydration and iron oxide does not form hydroxide or hydrates. This calculation resulted in calculated values of % $Ca(OH)_2$ greater than 100%. A reason for values over 100% may be that part of the lime gained weight by carbonation. This is discussed in a later section.

As the time of exposure to moisture increased, the samples first showed slow disintegration and then gradually turned into piles of loose powder. At the end of the

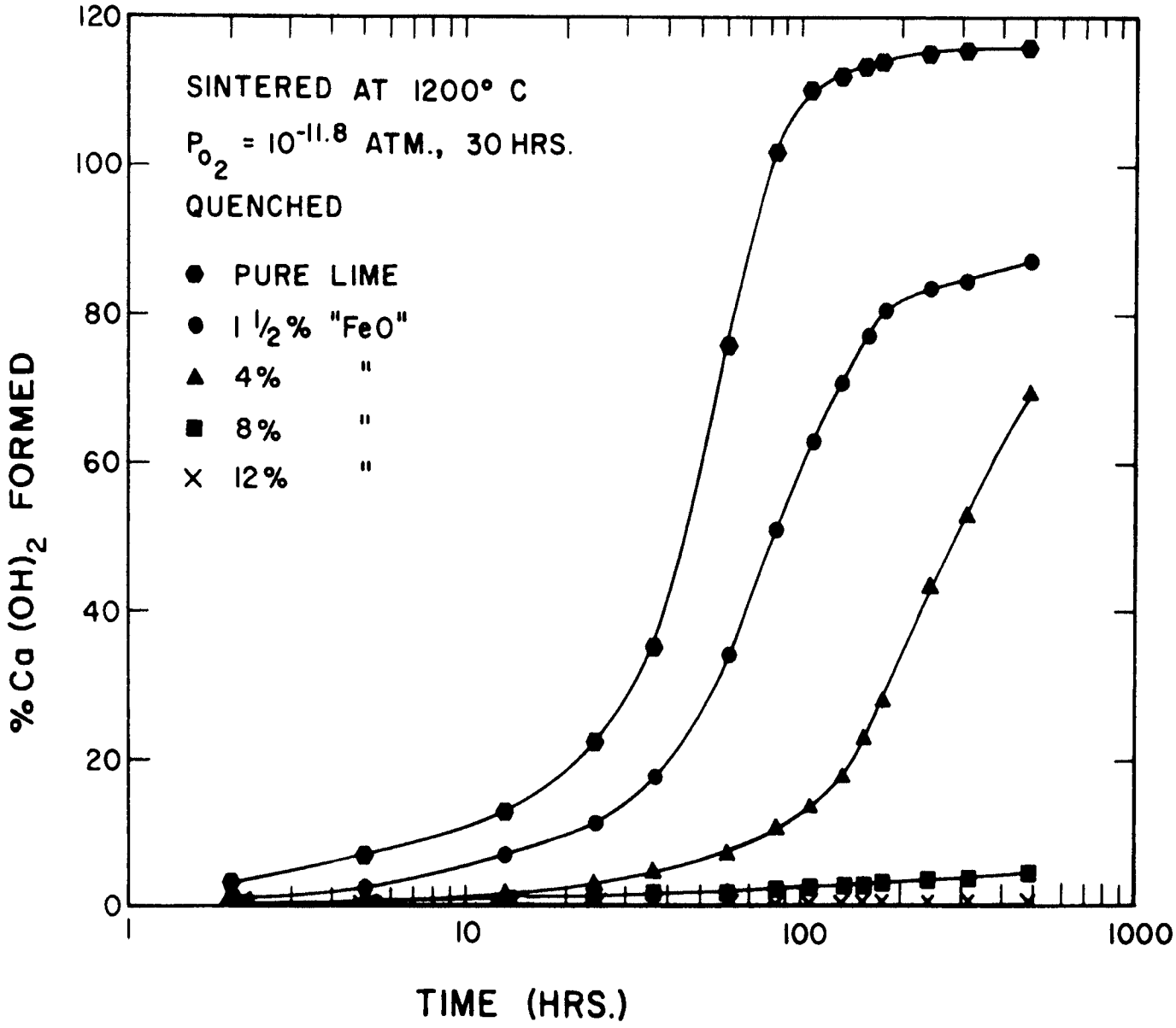

Figure 11(a). Hydration of CaO and CaO-Iron Oxide Mixtures.

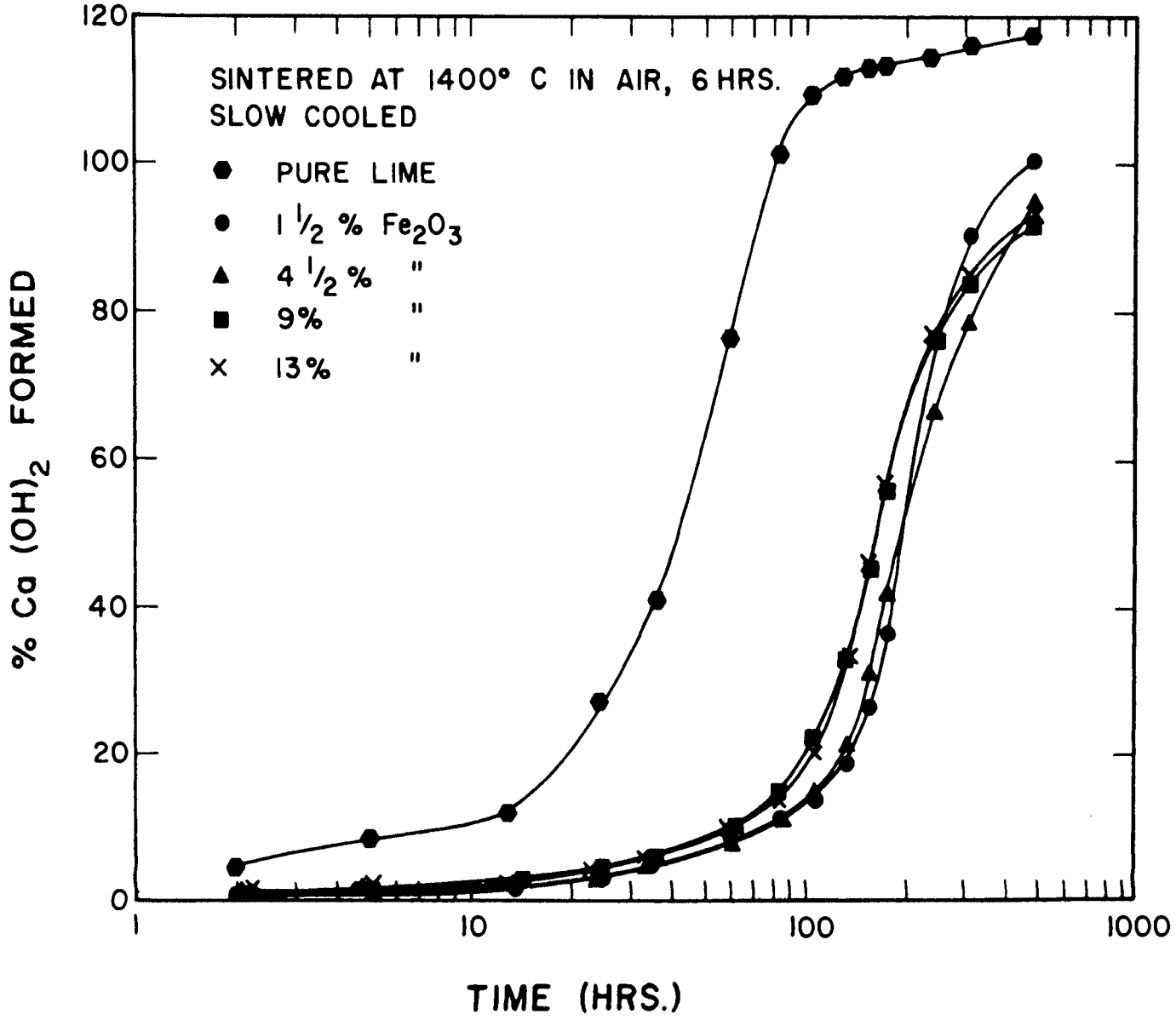

Figure 11(b). Hydration of CaO and CaO-Iron Oxide Mixtures.

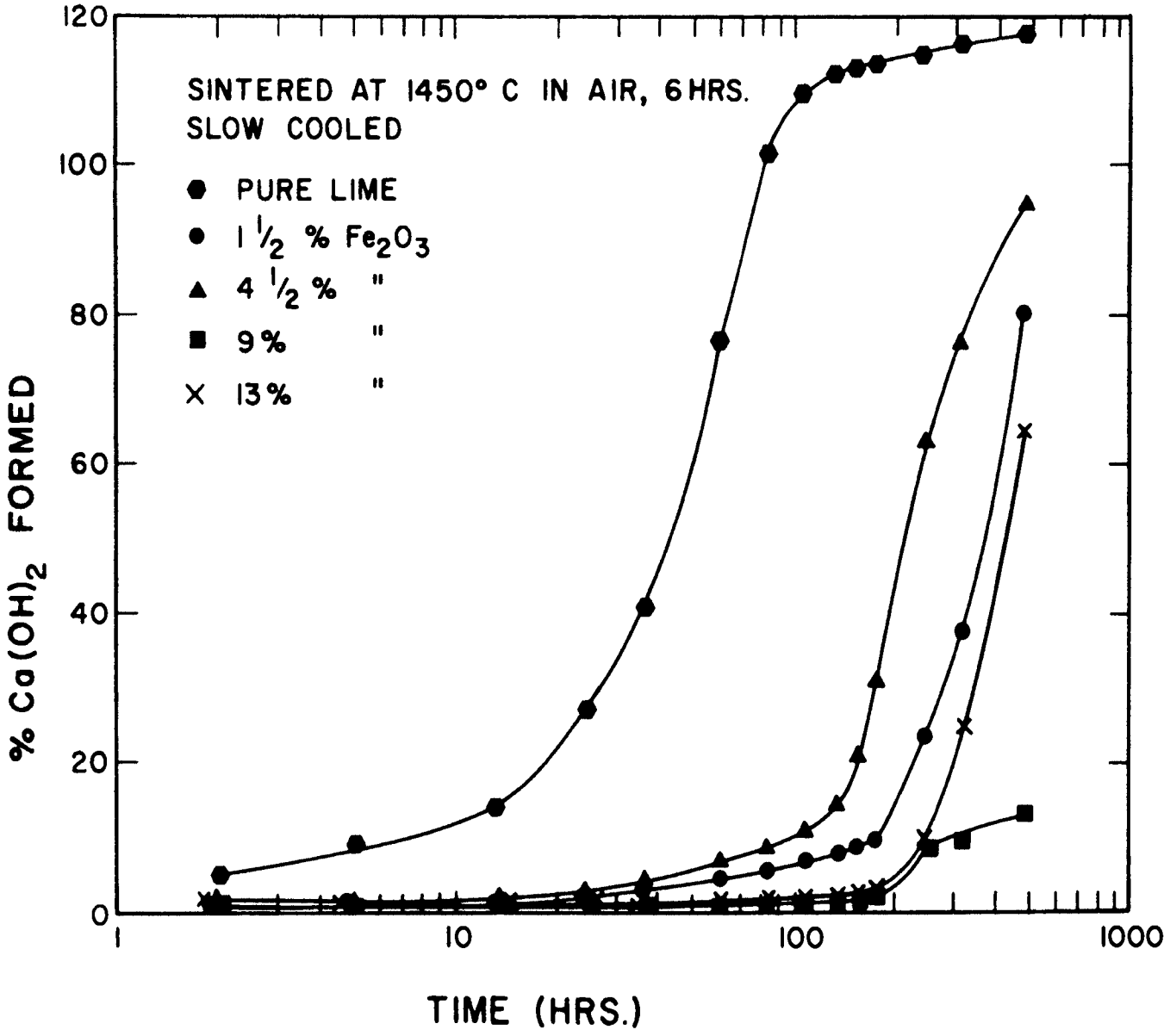

Figure 11(c). Hydration of CaO and CaO-Iron Oxide Mixtures.

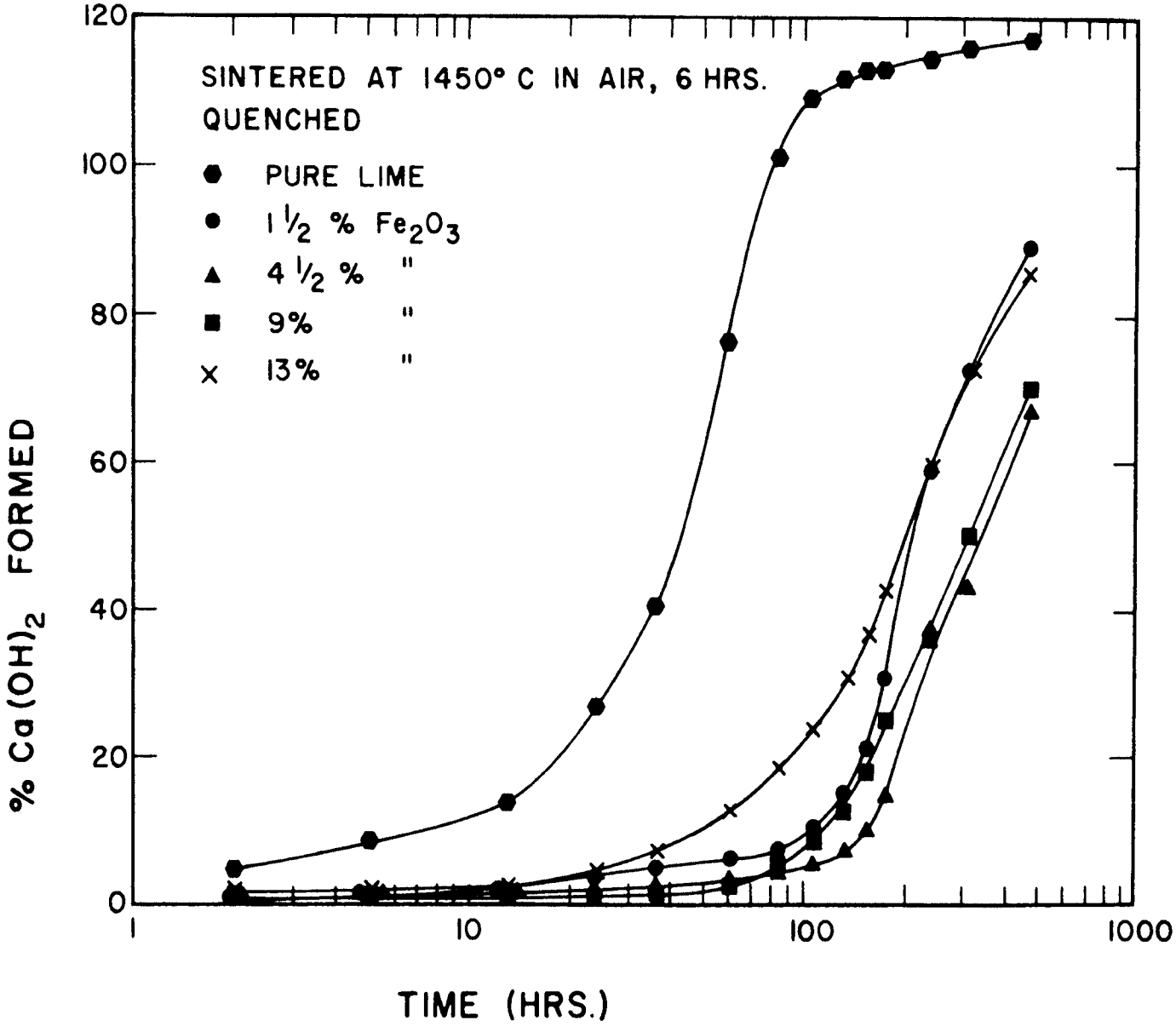

Figure 11(d). Hydration of CaO and CaO-Iron Oxide Mixtures.

hydration run, all but 3 samples disintegrated to piles of powder. The powders were colored from white to dark purple in the order of increasing iron oxide content.

The 3 samples which showed the greatest resistance to hydration are S1-4, S1-5 and S3-3. Two of these samples, S1-4 and S3-3, disintegrated to several pieces and only a small part of them became powder. Sample S1-5 did not show any change at all.

The samples were exposed to moist air for an accumulated time of 481 hours. This time was believed sufficient to distinguish the relative hydration behavior of the samples even though some of the samples had not completely hydrated.

As shown in Figs. 11(a) through 11(d), samples containing iron oxides generally exhibit lower rates of hydration than those of pure lime. But they reflect quite different behaviors toward hydration according to the sintering methods. The hydration behaviors of these samples are discussed in more detail, in a later section, in terms of phases present.

B. Discussion of Results

1. Measurement of the Melting Temperature of Dicalcium Ferrite in the Presence of Excess Lime

The melting temperature curve of $2CaO \cdot Fe_2O_3$ (in the presence of lime) shown in Fig. 8 does not show a linear relationship between log pO_2 and $1/T^{\circ}K$(melting) over the entire temperature range from 1200° to 1438°C. This is in contrast to a plot of the same variables for the redox reac-

tions of simple reducible oxides. For example:

$$2MO \longrightarrow 2M + O_2 \qquad (2)$$

$$\log K_2 = 2\log a_M + \log pO_2 - 2\log a_{MO}$$

Where a_{MO} and a_M are activities of MO and M, respectively. Taking the standard state as pure MO and pure M,

$$\log K_2 = \log pO_2$$

$$\frac{d(\Delta F^o/T)}{d(1/T)} = \frac{d(-RT\ln K_2/T)}{d(1/T)} = -2.3R \frac{d(\log pO_2)}{d(1/T)} = \Delta H^o$$

In this case a plot of log pO_2 vs. 1/T usually shows a nearly straight line, and this makes the calculation of ΔH^o possible.

In the present work, the melting reaction of this specific mixture is not a simple redox reaction as above. However, a semi-quantitative approach to treat such melting behavior may be considered as follows: CaO is not reducible under the oxygen partial pressures used in the present work. Hence the reducible oxide is the Fe_2O_3 combined as $2CaO\cdot Fe_2O_3$.

$$Fe_2O_{3(s)} \longrightarrow 2FeO_{(s,l)} + \tfrac{1}{2}O_2 \qquad (3)$$

$$\log K_3 = 2\log a_{\text{"FeO"}} + \tfrac{1}{2}\log pO_2 - \log a_{Fe_2O_3} \qquad (3a)$$

Where $a_{Fe_2O_3}$ and $a_{\text{"FeO"}}$ stand for activities of Fe_2O_3 and "FeO", respectively. Taking the standard state of Fe_2O_3 as pure Fe_2O_3, and of "FeO" as wustite or liquid iron oxide in equilibrium with metallic Fe; then, in equation (3a), the activity of Fe_2O_3 is fixed by the $CaO\text{-}2CaO\cdot Fe_2O_3$ equilibrium of reaction (4):

$$2CaO_{(s)} + Fe_2O_{3(s)} \longrightarrow 2CaO\cdot Fe_2O_{3(s)} \qquad (4)$$

$$\log K_4 = \log a_{2CaO\cdot Fe_2O_3} - 2\log a_{CaO} - \log a_{Fe_2O_3}$$

Where $a_{2CaO\cdot Fe_2O_3}$ and a_{CaO} represent activities of $2CaO\cdot Fe_2O_3$

and CaO, respectively. Taking the standard states as pure $2CaO \cdot Fe_2O_3$ and pure CaO, then,

$$\log K_4 = -\log a_{Fe_2O_3} \qquad (4a)$$

Substitute (4a) into (3a), then,

$$\log K_3 = 2\log a_{"FeO"} + \tfrac{1}{2}\log pO_2 + \log K_4$$

$$\log (K_3/K_4) = 2\log a_{"FeO"} + \tfrac{1}{2}\log pO_2$$

Let $K_3/K_4 = K_5$, then,

$$\log K_5 - 2\log a_{"FeO"} = \tfrac{1}{2}\log pO_2$$

$$\frac{2\log K_5 - 4\log a_{"FeO"}}{1/T} = \frac{\log pO_2}{1/T}$$

Therefore, the curve in Fig. 8 is actually a plot of $2\log K_5 - 4\log a_{"FeO"}$ vs. $1/T$, where T is the temperature where CaO(ss), dicalcium ferrite, liquid, and gas coexist. At low pO_2, when iron in the liquid exists almost entirely as Fe^{++} and $a_{"FeO"}$ is nearly one, then, $(2\log K_5 - \text{small number})/(1/T) \longrightarrow 2\log K_5/(1/T)$. The resulting plot will be close to a straight line. At higher pO_2, $a_{"FeO"} \longrightarrow 0$ as pO_2 increases past one atm, since the iron in the liquid exists almost exclusively as Fe^{+++}. As the oxygen pressure increases past 1 atm, then, $(2\log K_5 - 4\log a_{"FeO"})/(1/T)$ approaches $+\infty$ and a plot of $\log pO_2/(1/T)$ will approach a vertical line. If the $a_{"FeO"}$ was actually vanishingly small, the melting temperature would be independent of the oxygen partial pressure. This state is approached above 1 atm O_2 pressure, as is clearly shown by the steep increase of the melting curve above an oxygen pressure of about 0.1 atm (see Fig. 8).

Dicalcium ferrite with excess CaO melted in air at 1438°C,

which is the same temperature given on Fig. 5. The melting point of stoichiometric $2CaO \cdot Fe_2O_3$ determined by Phillips and Muan[11] in air and at 1 atm O_2 pressure are also plotted in Fig. 8. These data are not sufficient to draw a curve of log pO_2 vs. 1/T(melting). There is a difference of about 11°C between the melting point of stoichiometric $2CaO \cdot Fe_2O_3$ and the melting temperature of $2CaO \cdot Fe_2O_3$ in the presence of excess CaO. As noted earlier, this difference should disappear at some lower, but as yet unknown pO_2.

The results of the present work can be compared to the oxygen potential diagram for the system Fe-Ca-O (Fig. 6) constructed by Turkdogan.[13] The part of his diagram pertinent to the present work is replotted in Fig. 12 as log pO_2 vs. temperature(°C). As shown in the diagram, the slope and position of the curve determined experimentally differs appreciably from that of his corresponding calculated curve R. Since 1200°C was the lowest temperature investigated in this work, Turkdogan's diagram in the vicinity of the invariant point VIII and IX could not be checked.

2. Determination of the Solubility Limits of Iron Oxide in Solid Lime

Figs. 9 and 10 show the profound influence of the oxygen pressure on the solubility of iron oxide in CaO at each temperature. The most carefully studied part of the diagram is the phase boundary between CaO(ss) and liquid oxide. Because of the relatively low stability of $2CaO \cdot Fe_2O_3$ at 1400°C, the range of the oxygen pressure for the coexistance of CaO(ss)

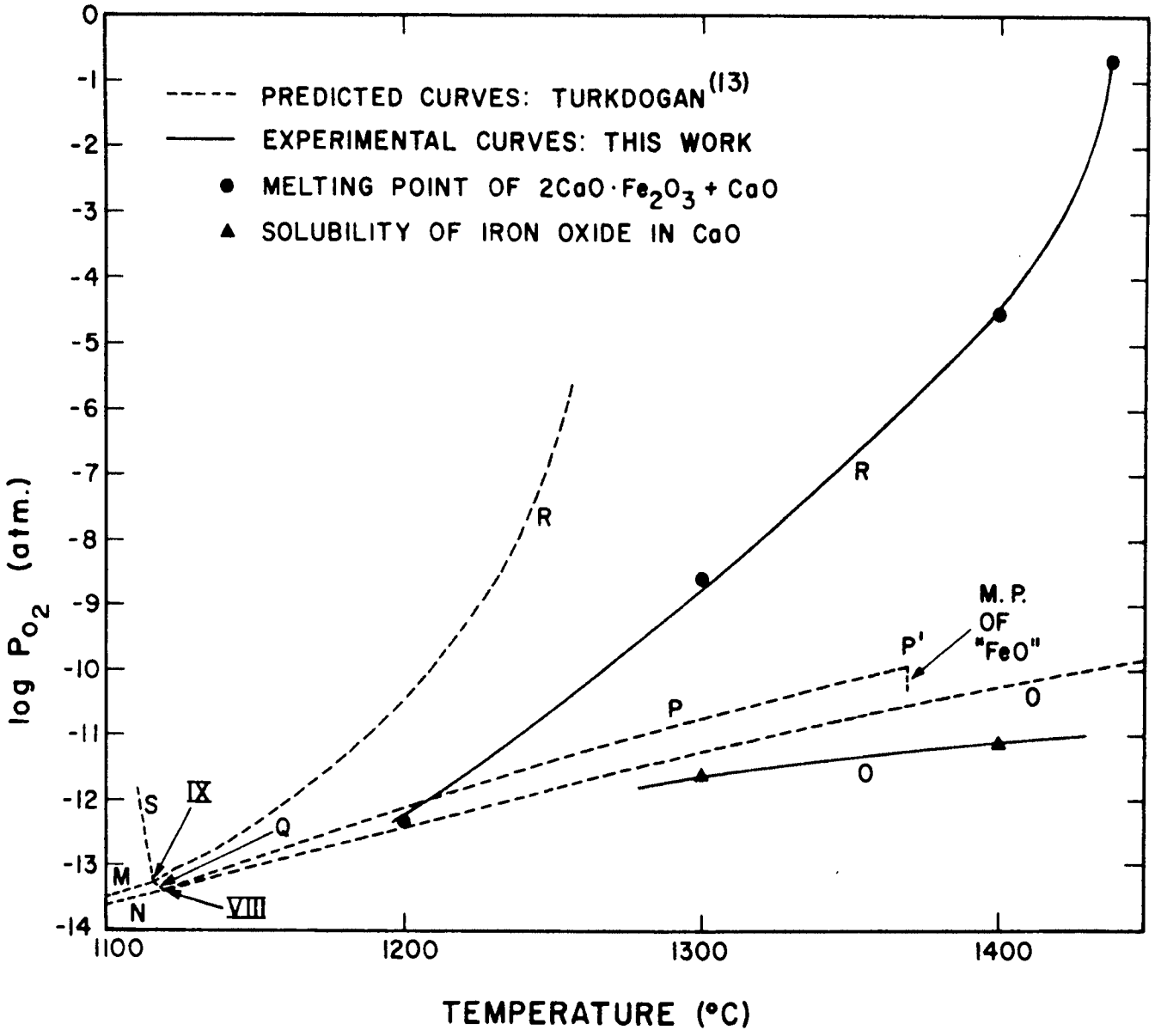

Figure 12. The Oxygen Pressure vs. Temperature Curve for the System Fe-Ca-O.

and liquid is much larger than that at 1300°C. The solubility curve clearly shows that lime dissolves a certain amount of iron oxide in solid solution under the given pO_2. For a sample containing more iron oxide than can be dissolved in the lime, either a liquid phase, $2CaO \cdot Fe_2O_3$ or metallic iron is present. The relationship between the temperature, composition, pO_2, and phases formed is important in understanding how lime might dissolve in an iron oxide slag, and this is discussed in a later section.

In order to show the effect of temperature on the solubility limits of iron oxide in lime, the solubility curves of Figs. 9 and 10 are reproduced in a slightly different way in Fig. 13. As seen from the diagram, the solubility of iron oxide in lime is lower at 1400°C than at 1300°C over the comparable oxygen pressure range. Therefore, it may be said that for a constant oxygen pressure, the solubility of iron oxide in CaO decreases as the temperature increases. From a consideration of these effects of temperature and oxygen pressure on the solubility limit of iron oxide in lime, a hypothesis can be proposed to account for the solution of lime in a BOF slag, as discussed later.

In Fig. 14, the maximum solubility limits of iron oxide in CaO of the present work at 1300° and 1400°C are compared with those of other investigators at the same temperature levels. The data of this work show excellent agreement with those estimated by Allen and Snow[2] on the basis of X-ray data. The largest discrepancy exists between this work and

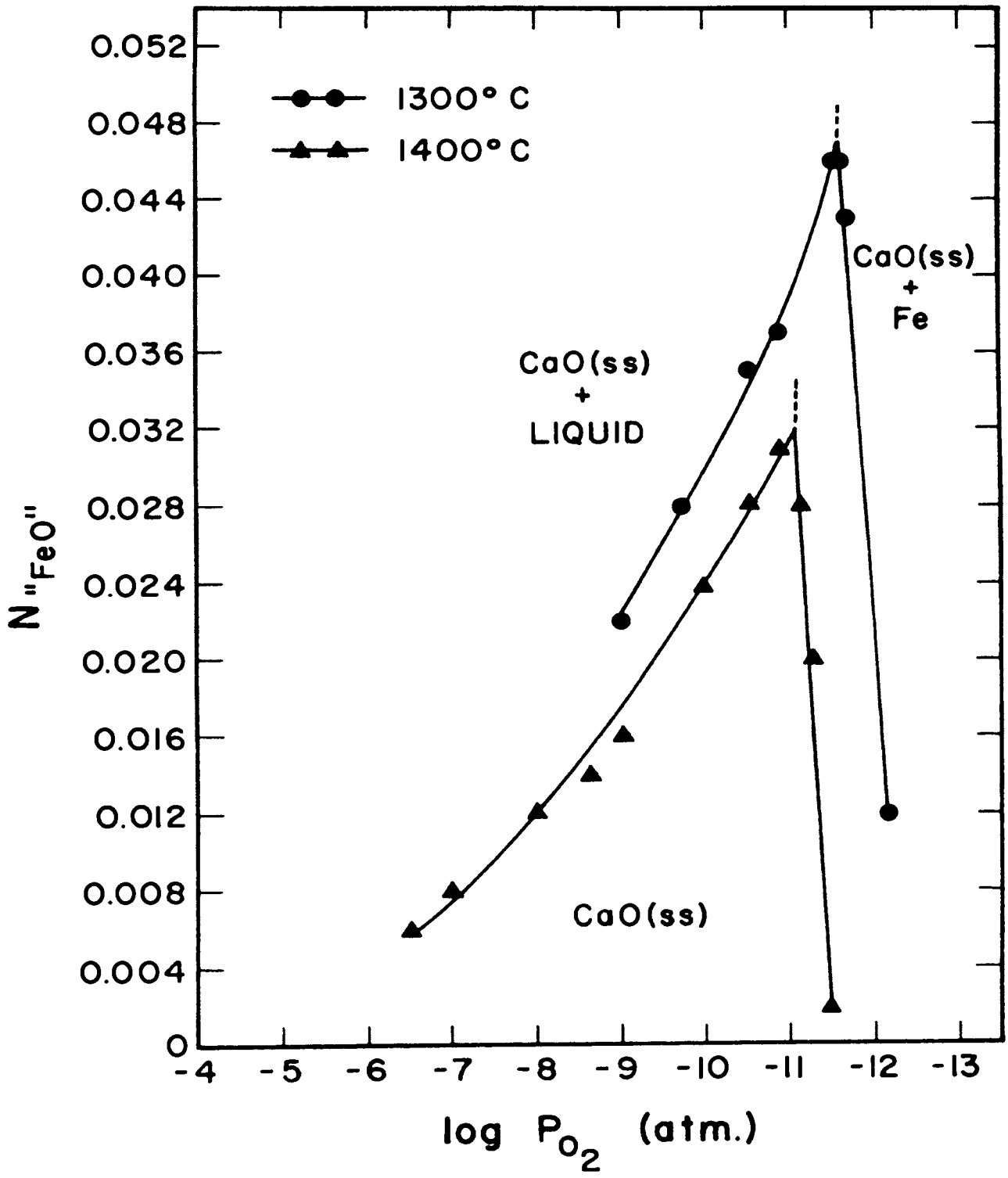

Figure 13. The Solubility of Iron Oxide in Solid Lime at 1300° and 1400°C.

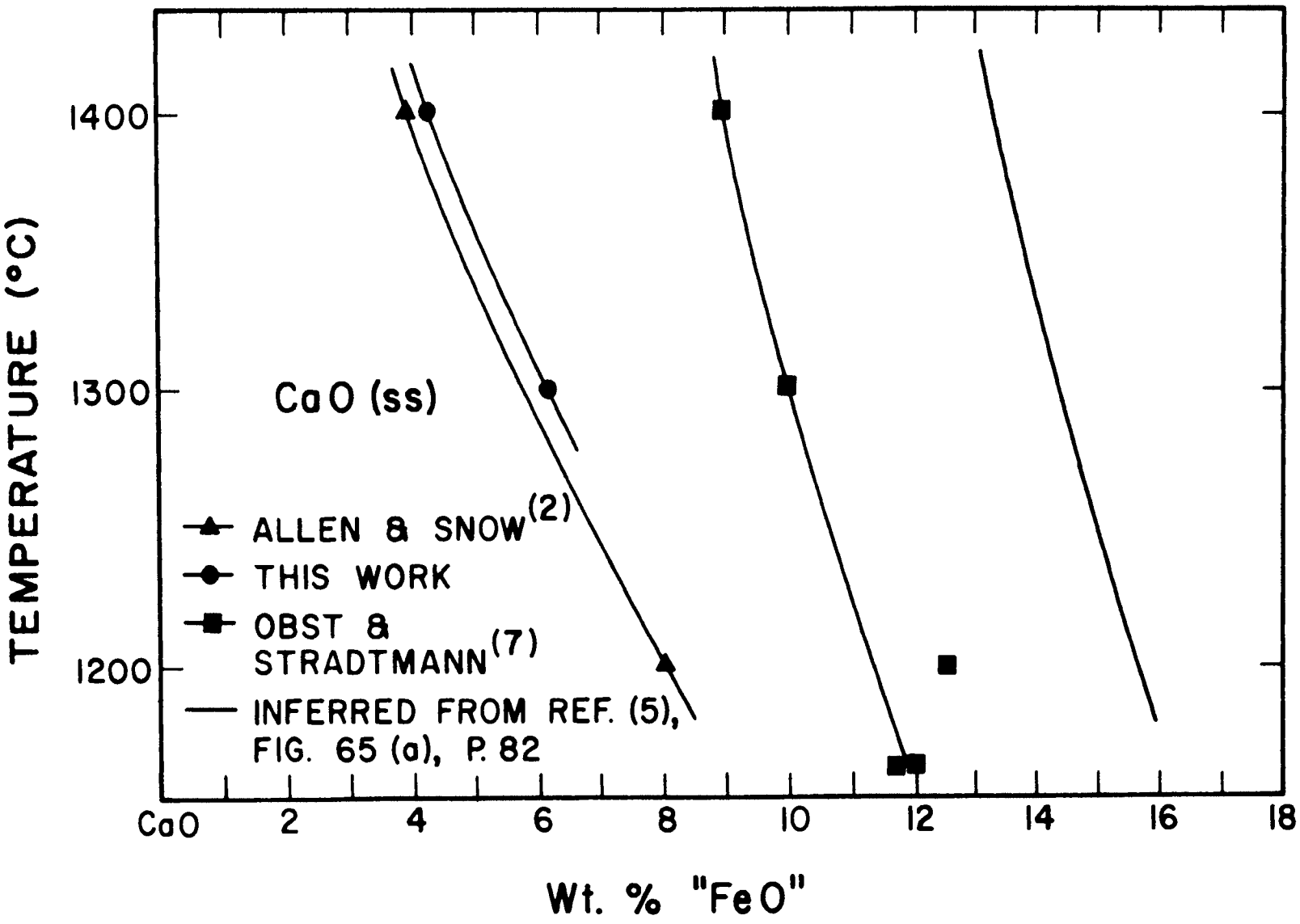

Figure 14. Comparison of Maximum Solubility of Iron Oxide in Solid Lime.

the diagram published by Muan and Osborn.[5] The data of Obst et al.[6,7] show solubility values about twice as high as the present results. The source of the difference is not clear. The experimental technique of electron microprobe analysis of lime particles used by Obst et al.[6] is not completely described in terms of their standard sample for iron.

The present data on maximum solubilities at 1300° and 1400°C are also plotted in Fig. 12 in comparison with the study of Turkdogan.[13] As shown in the diagram, the present results show a lower oxygen pressure for curve O than his calculated univariant curve O. The results of the present study indicate that the other univariant curves drawn by Turkdogan[13] also need experimental verification.

Besides the quantitative comparisons between the present data and data previously published on the system CaO-"FeO" or Fe-Ca-O, the data may be used to suggest a hypothesis for the mechanism of lime solution in a BOF slag. This is done by taking into account the interactions between CaO, and iron oxide and SiO_2 as the temperaure increases. The lime added into a BOF vessel will most likely react simultaneously with iron oxide and SiO_2 which are formed as a slag right after the oxygen blowing begins. The outer part of the lime particle reacts with this slag to form CaO(ss) and $2CaO \cdot SiO_2$. The silicate may eventually form a sort of "shell" around the lime particle, which greatly retards further reaction between lime and slag. Since this occurs at the initial

blowing stage, the slag temperature is still low, so the solubility of iron oxide in CaO is rather high. As the slag temperature rises, however, the inner layer of CaO(ss) becomes supersaturated with iron oxide, because of its lower solid solubility at high temperature. A liquid will form, and this liquid should weaken the bond between lime and the outer $2CaO \cdot SiO_2$ shell. Then in the turbulence of the bath, the silicate shell may readily crack or spall off, so that a fresh lime surface will be exposed to the slag, thereby aiding the dissolution process.

This hypothesis is in agreement with the findings of a layer of CaO(ss) on the ouside of lumps of lime taken from an operating BOF.[7,21,30,34] It also indicates that isothermal lime/slag dissolution studies may not be taking into account an important step in the actual dissolution mechanism. The data also show conditions under which prereacted mixtures of lime and iron oxide would form a liquid phase, when heated in the BOF.

3. Hydration Tests on Lime and Mixtures of Lime-Iron Oxides

As mentioned ealier, calculations of the percent hydration of lime yielded values higher than 100%. This indicates that the increase in sample weight comes not only from hydration but also from some other reaction. The most likely reaction is that of carbonation.

In the hydration runs, the samples were exposed to laboratory air for about an hour at each weighing. In addi-

tion to the usual small CO_2 content in normal air, CO_2 was used in the laboratory for atmosphere control. At the end of the hydration runs, the total time of sample exposure to air was 14 hours. Thus the opportunity existed for the lime to react with CO_2 by either of the following reactions:

$$CaO + CO_2 \rightarrow CaCO_3 \quad (5)$$

$$Ca(OH)_2 + CO_2 \rightarrow CaCO_3 + H_2O \quad (6)$$

It is well known in the literature[42-44] that normal air slaking of lime involves both hydration and carbonation.

If the ratio of carbonated lime to hydrated lime was 1 to 9, for example, calculations of % hydration, based entirely on equation (1), would give a value of 115% lime hydrated, which is very close to the final values calculated from the data on the pure lime samples.

In an attempt to confirm the carbonation hypothesis, a qualitative test was performed on the hydrated samples at the end of the run. A small amount of each hydrated sample was immersed into water in a test tube, and then followed by a few drops of dilute HCl. The samples which had gained more than 100% hydration evolved some gas bubbles, whereas other samples did not show any gas evolution. The bubbles were probably CO_2 generated by the following chemical equation:

$$CaCO_3 + 2HCl \rightarrow CaCl_2 + H_2O + CO_2 \quad (7)$$

This is good confirmation that hydration values over 100% are due to carbonation of part of the samples.

As indicated previously, the samples containing iron oxides in Figs. 11(a) through 11(d) showed various rates of

hydration. There are several difficulties in explaining such hydration behavior in detail, because of the limited test results. However, some conclusions can be made by correlating the results with the appropriate phase diagram, and the following observations.

a) When iron oxide is added to CaO, one of the reaction products is CaO(ss). The solubility of iron oxide in solid CaO varies according to the sintering conditions, but in any case, the more iron oxide in CaO(ss) the lower the activity of CaO in CaO(ss).[4,8] It seems reasonable that lime which has a low activity has a decreased tendency to react with moisture.

b) When more iron oxide is added to lime than it can dissolve, the reaction product is either liquid oxide or $2CaO \cdot Fe_2O_3$ according to the sintering condition.* The amount of these phases present increases with increasing amount of iron oxide. It is believed that these phases do not take part in hydration at room temperature,[45] or take part only very slowly. Hence the formation of these phases lowers the amount of free lime in the sample (on the basis of total CaO) in proportion to the amount of the liquid or $2CaO \cdot Fe_2O_3$ present.

c) It has been found that impurities in oxides play a

---

*Metallic iron could also form if the pO_2 during sintering was very low, but this was not the case for any of the samples investigated in this part of the work.

significant role in increasing the sintering rate.[46-49] It seems that the presence of Fe_2O_3 increases the sintering rate of the lime so that the pellets containing Fe_2O_3 have a higher density than pure lime. This higher density retards the access to, and penetration of moisture into the sample. Although the role of impurities in affecting the rate of sintering is not well known, it seems that small amounts of impurities (up to the limit of solid solubility) are often just as effective, if not more so, than large amounts, in accelerating the rate of sintering.

d) It is well known that the presence of a liquid phase during sintering causes increased densification of the compact.[49-52] The liquid phase fills the pores and encloses the lime particles, so that the surface area of the lime in the sample is substantially reduced.

e) The solidification behavior of liquid in the sample depends on the rate of cooling. Many fine interlocking glass-like particles may be formed, or coarse crystalline phases may prevail. It was observed that the samples quenched in air or into alcohol contained many fine cracks, even though the samples were intact. Because of the random nature of the cracks, and the nature of the liquid devitrification product, the actual surface area and type of surface exposed to moisture varied from sample to sample. The surface area is one of the more important factors contributing to the rate of hydration.

In Fig. 11(a), pure lime shows the most rapid $Ca(OH)_2$

formation, while the lime-iron oxide solid solutions show a general relationship between decreasing hydration rate and increasing iron oxide content of the sample. This tendency has also been shown by Timucin and Morris,[53] who have obtained similar results by air slaking of various lime-iron oxide solid solutions. A noticeable feature that appears in Fig. 11(a) is that the sample containing 12% iron oxide (S1-5) did not gain any weight in 481 hours, even though the pure lime sample had achieved complete hydration. Such a hydration behavior may be explained by the effects of a), b) and d).

In Fig. 11(b), the rates of hydration of the samples containing Fe_2O_3 are relatively slow compared with that of pure lime. But despite the slow rate, hydration of the samples proceeds gradually toward completion. There seems to be no general trend between the rates and the amount of iron oxide. These behaviors of the samples may be due to the effects of b), c) and e).

The two sets of samples (S3 and S4) sintered at 1450°C in air (Figs. 11(c) and 11(d)) show considerably slower rates of hydration compared to those of samples sintered at 1400°C (Fig. 11(b)). Even though the rates of hydration of these samples are very slow, hydration proceeds steadily. However, the hydration data do not indicate any consistent relationships either between the rates and Fe_2O_3 content or between the rates and quenching methods. Such a hydration behavior of the samples may be explained by the effects of b), c), d)

and e).

As shown in Figs. 11(a) and 11(b), there seems to be no appreciable difference in the rate of hydration between pure lime samples (S1-1 and S2-1) which were prepared at different sintering conditions. The reason may be explained by relating the sintering condition to the physical properties of the limes. There are various factors which influence the rate of hydration.[42,43,54] All factors, except the second-stage sintering treatment, are identical for both samples. The behavior of these limes toward hydration may be that: i) The second stage treatment was not sufficient to change the physical properties of lime after the first treatment of calcining, or ii) The change in physical properties was about the same for the second stage of sintering (30 hours at 1200°C vs. 6 hours at 1400°C). Even though the above explanations may not involve all the factors which influence the rate of hydration, the results of the hydration tests indicate that:

1) The presence of iron oxide (up to 13% Fe_2O_3) in a CaO pellet increases the resistance of lime to atmospheric hydration.

2) The effect of iron oxide on the resistance of lime is more pronounced when the lime contains iron oxide in the form of solid solution.

3) The highest resistance of lime is obtained when, during sintering, the lime consists of iron oxide-saturated solid solution and a small amount of liquid oxide. This

agrees well with the observations of Allen and Snow.[2] They reported that CaO(ss) containing 10% iron oxide did not hydrate at all for 4 months.

Samples having a high hydration resistance would probably show a low reactivity with water.[2,53] However, as discussed by Obst et al.,[7,30,34] pure lime dissolves slower in an iron oxide slag than CaO(ss) does. For lime containing iron oxide, the inconsistancy between its water reactivity and its dissolution rate in slag was pointed out by these authors, and by Limes and Russell.[28] Some new room temperature test would be very helpful if it could predict the dissolution rate of lime containing iron oxides in typical BOF slags.

In view of importance of lime as a major fluxing material in the BOF process, the following advantages could be expected if a lime-iron oxide solid solution was used instead of pure lime; a) faster slag formation and smoother operation, b) higher dissolved CaO in slag, and less undissolved CaO, c) decreased amount of H_2 in steel which originates as H_2O in the flux lime, and d) minimized problems of flux lime hydration during storage and transportation. Some of the above factors have been discussed by Obst et al.,[27,30,55] Schlitt,[33] Snyder[56] and Derge.[57]

C. Suggestions for Further Study

Measurement of the melting temperature as a function of oxygen pressure of $2CaO \cdot Fe_2O_3$ with excess lime needs more work at temperatures below 1200°C together with microscopic

examination of quenched samples at each melting temperature. This would determine the exact location of the univariant curve R; and clarify the published discrepancies in the extent of the stability region of $2CaO \cdot Fe_2O_3$, that appear in the phase diagrams of Allen and Snow[2] and Tromel, Jager and Schurmann.[3]

By determining the composition of the liquid phase present with lime at each oxygen pressure, the phase boundary of liquid saturated with lime would be fixed.

A determination of the Fe^{+++}/Fe^{++} ratio at the lime-rich end of the phase diagram would establish the effect of lime on the relative stabilities of ferric and ferrous iron, in both the solid and liquid phases. This data is known only above 45% "FeO" in Fig. 1. Furthermore, a careful review of the work of Allen and Snow[2] fails to show the experimental temperature and the basis of calculation for the weight % Fe_2O_3 given in Fig. 7 in their work. The determination of Fe^{+++}/Fe^{++} ratio would also be helpful in understanding the upper portion of Fig. 1.

An examination of the rate of solution of pure lime, and lime containing different amounts of dissolved iron oxide in synthetic BOF slags would provide useful information for the practical application of the results of this study.

Further hydration test on additional samples would give a better understanding of the hydration behavior of lime as related to sintering conditions and rate of quenching. Samples of iron-oxide saturated CaO(ss), liquid oxide and

$2CaO \cdot Fe_2O_3$ should be prepared at various temperatures and oxygen pressures, to see if these substances participate in the hydration reaction. These results in relation to the solubility limit data could be used to determine optimum composition and sintering condition for the production of lime with mixtures of iron oxide.

V. SUMMARY AND CONCLUSIONS

The present study consisted of three distinct types of experiments: 1) Determination of the solubility limits of iron oxide in solid lime as a function of oxygen pressure at 1300° and 1400°C; 2) Measurement of the melting temperature of dicalcium ferrite in the presence of excess lime, as a function of oxygen pressure; and 3) Hydration tests on lime and sintered mixtures of lime plus iron oxide.

The effect of oxygen pressure on the solubility limits of iron oxide in CaO was profound at both temperatures. Within the oxygen pressure range where lime-iron oxide solid solution and liquid are compatible, the solubility limits of iron oxide in CaO were increased with decreasing oxygen partial pressures. The maximum solubility of iron oxide in CaO was found to be about 6.2% "FeO" at $pO_2 = 10^{-11.60}$ atm at 1300°C and about 4.2% "FeO" at $pO_2 = 10^{-11.10}$ atm at 1400°C. The stability region of $2CaO \cdot Fe_2O_3$ was much smaller at 1400°C than at 1300°C. The solubility limit of iron oxide in CaO was decreased with increasing temperature.

Pellets of pure lime and mixtures of lime plus iron oxide were sintered for various times and temperatures at controlled pO_2, and exposed to moist air with a constant relative humidity of about 43% at 25°C. The weight gain of each sample was checked at appropriate time intervals. The results of hydration experiments showed that iron oxide in lime retards the rate of hydration. The greatest resistance to

hydration was exhibited by a sample sintered to give a lime-ferrous oxide solid solution and liquid, which did not hydrate at all during the test.

The phase diagrams can be used to interpret the results obtained from examination of partly dissolved lime taken from real or synthetic BOF slags. A mechanism is suggested for the dissolution of lime with increasing temperature in a BOF-type slag.

BIBLIOGRAPHY

1. V. Cirilli and A. Burdese: "The Calcium Oixde-Wustite System." In 2nd Int. Sym. React. Solids 1952 (Gothenburg: Elanders Boktrykeri Akhebolag. 1954), pp. 867-879.

2. W. C. Allen and R. B. Snow: "The Orthosilicate-Iron Oxide Portion of the System CaO-FeO-SiO_2." J. Am. Cer. Soc., 1955, vol. 38, pp. 264-280.

3. Tromel, W. Jager and E. Schurmann: "Investigations in the System Iron-Iron Oxide-Lime." Arch. Eisenhuttenw. 1955, vol. 26, pp. 687-700.

4. W. C. Hahn, Jr.: "Studies of the Thermodynamic Properties of Oxide Solid Solutions" Ph.D. Thesis, The Pennsylvania State University, 1960.

5. A. Muan and E. F. Osborn: Phase Equilibria Among Oxides in Steelmaking, Addison-Wesley Publishing Co., Reading, Massachusetts, 1965, pp. 81-82.

6. K. H. Obst, H. C. Horn and J. Stradtmann: "A Study on the Solid State Phase Equilibria in the System CaO-FeO_n as an Example of the Application of the Electron Beam Microanalyser." Mikrochim. Acta (Wien), Suppl. III., 1968, pp. 147-154.

7. K. H. Obst and J. Stradtmann: "The Calcium Oxide-Ferrous Oxide System as a Basis for the Study of the Dissolution of Lime in Steelmaking." Arch. Eisenhuttenw., 1969, vol. 40 pp. 615-617. (Brutcher Translation No. 7928)

8. R. E. Johnson and A. Muan: "Activity-Composition Relations in Solid Solutions of the System CaO-FeO-SiO_2 in Contact with Metallic Iron at 1080°C." Trans. AIME, 1967, vol. 239, 1931-1939.

9. H. Fujita, Y. Iritani and S. Maruhashi: "Activities in Iron Oxide-Lime Slags." Tetsu-to-Hagane, 1968, vol. 54, pp. 359-370.

10. M. F. Koehler, R. Barany and K. K. Kelley: "Heats and Free Energies of Formation of Ferrites and Aluminates of Calcium, Magnesium, Sodium, and Lithium." U.S. Bureau of Mines Rept. of Investigations, No. 5711, 1961.

11. B. Phillips and A. Muan: "Phase Equilibria in the System CaO-Iron Oxide in Air and at 1 atm O_2 Pressure." J. Am. Cer. Soc., 1958, vol. 41, pp. 445-454.

12. B. Phillips and A. Muan: "Stability Relations of Calcium Ferrites: Phase Equilibria in the System $2CaO \cdot Fe_2O_3$-$FeO \cdot Fe_2O_3$-Fe_2O_3 Above 1135°C." Trans. AIME, 1960, vol. 218, pp. 1112-1118.

13. E. T. Turkdogan: "Oxygen Potentials and Phase Equilibria in the Fe-Ca-O System." Trans. AIME, 1961, vol. 221, pp. 546-553.

14. D. A. Reeve and A. G. Gregory: "Modifications of the Oxygen Potential Diagram for the System Fe-Ca-O." Trans. Instn. Min. Metall, (Sect. C: Mineral Progress. Extr. Metall.), 1967, vol. 76, pp. c273-c277.

15. 1968 Book of ASTM STANDARDS with Related Material, Part 9, Cement, Lime, Gypsum, c-110, Sec. 20-22, pp. 88-90.

16. J. Wuhrer: "On the Reactivity of Lime from Different Kiln Systems." Pamphlet, Published by National Lime Association, Washington, D.C., 1965.

17. K. F. Behrens, J. Koenitzer and T. Kootz: "The Effect of Lime Properties on Basic Oxygen Steelmaking." J. Metals, 1965, vol. 17, pp. 776-784.

18. J. A. Gregory, A. Schrader, R. Bashford and F. G. Hubbard: "Basic Oxygen Steelmaking Flux: an Examination of Water Activity and Digestion to a Slag." J. Iron and Steel Inst., 1965, vol. 203, pp. 886-891

19. R. W. Limes: "Refractories for Basic Oxygen Furnaces." Open Hearth Proceedings, 1966, vol. 49, pp. 192-202.

20. R. O. Russell: "Lime Reactivity and Solution Rates." J. Metals, 1967, vol. 19, Aug., pp. 104-106.

21. G. Konig, H. Rellermeyer and K. H. Obst: "Processes Taking Place in the Dissolution of Hard and Soft-Burnt Lime in the Slags from the Basic Oxygen Furnace." Stahl u. Eisen, 1967, vol. 87, pp. 1071-1077. (Brutcher Translation No. 7264)

22. F. Reinders, E. Friedl, and G. Kauder: "Operating Results on Lime with Different Degrees of Calcination in the Basic Oxygen Process" Stahl u. Eisen, 1969, vol. 89, pp. 57-63. (Brutcher Translation No. 7724).

23. F. Bardenheuer, H. vom Ende, and P. C. Oberhauser: "Lime Dissolution, Slag Practice, and Life of Dolomite Lining when Blowing Low-Phosphorus Hot Metal in the Basic Oxygen(LD) Furnace." Stahl u. Eisen, 1968, vol. 88, pp. 1285-1290. (Brutcher Translation No. 7671)

24. F. Bardenheuer, H. vom Ende and K. G. Speith: "Contribution to the Metallurgy of the "LD" Process." Blast Furnace and Steel Plant, 1970, vol. 58, pp. 401-407.

25. L. A. Leonard: "Influence of Lime Quality on Oxygen Steelmaking." J. Iron and Steel Inst., 1970, vol. 208, pp. 324-328.

26. L. C. Anderson and J. Vernon: "The Quality and Production of Lime for Basic Oxygen Steelmaking." J. Iron and Steel Inst., 1970, vol. 208, pp. 329-335.

27. K. H. Obst, J. Stradtmann, W. Ullrich and G. Konig: "Present Status and Technical Advances of Steelworks Lime for Basic Oxygen Furnace in Germany." The Reaction Parameters of Lime, ASTM STP 472, Am. Soc. for Test. and Matl., 1970, pp. 173-192.

28. R. W. Limes and R. O. Russell: "Crucible Test for Lime Reactivity in Slags." The Reaction Parameters of Lime, ASTM STP 472, Am. Soc. for Test. and Matl., 1970, pp. 161-172.

29. W. J. Schlitt and G. W. Healy: "Characterization of Lime: A Comparison and Scaling Down of the Coarse Grain Titration Test and the ASTM Slaking Rate Test." The Reaction Parameters of Lime, ASTM STP 472, Am. Soc. for Test. and Matl., 1970, pp. 143-160.

30. K. H. Obst and J. Stradtmann: "The Importance of Lime Quality in Steelmaking." Blast Furnace and Steel Plant, 1969, vol. 57, pp. 933-938.

31. R. D. Pehlke and P. F. Klaas: "Kinetics of Lime Solution in Basic Oxidizing Slags." ORA Project 05907, Final Report, Aug. 1966, The University of Michigan, College of Engineering, Ann Arbor, Michigan.

32. R. J. Leonard, Jr.: "Kinetics of Calcium Oxide Dissolution in Iron Oxide-Calcium Oxide Liquids." Ph.D. Thesis Rutgers University, 1967.

33. W. H. Schlitt, III: "The Dissolution of Lime in Calcium-Iron Silicate Slags at 1375°C." Ph.D. Thesis, The Pennsylvania State University, 1968.

34. K. H. Obst, J. Stradtmann and H. C. Horn: "Electron Microprobe Study (of Slag Formation)." Mikrochim. Acta (Wien), Suppl. III., 1968, pp. 140-146.

35. G. Derge and J. R. Shegog: "Observations on the Solution of Calcium Oxide in Slag Systems." The Reaction Parameters of Lime, ASTM STP472, Am. Soc. for Test. and Matl., 1970, pp. 132-142.

36. R. A. Robie and D. R. Waldbaum: "Thermodynamic Properties of Minerals and Related Substances." U.S. Geol. Surv. Bull. 1259, 1968, pp. 100-101.

37. L. S. Darken and R. W. Gurry: "The System Iron-Oxygen. I. The Wustite Field and Related Equilibria." J. Am. Chem. Soc., 1945, vol. 67, pp. 1398-1412.

38. M. Timucin: "Phase Equilibria and Thermodynamic Studies in the System $CaO-FeO-Fe_2O_3-SiO_2$." Ph.D. Thesis, The University of Missouri-Rolla, 1969.

39. R. C. Weast (Ed.): Handbook of Chemistry and Physics, Chemical Rubber Co., Cleveland, Ohio, 1969-1970 (50th Edition), p. B-100.

40. N. A. Lange (Ed.): Handbook of Chemistry, Handbook Publisher's, Inc., Sandusky, Ohio, 1956 (9th Edition), pp. 1420-1422.

41. L. S. Darken and R. W. Gurry: "The System Iron-Oxygen. II. Equilibrium and Thermodynamics of Liquid Oxide and Other Phases." J. Am. Chem. Soc., 1946, vol., 68. pp. 798-816.

42. R. S. Boynton: Chemistry and Technology of Lime and Limestone. Interscience Publishers, New York, 1966, pp. 165-200, 287-321.

43. N. V. S. Knibbs: Lime and Magnesia, Ernest Benn Ltd., London, 1924, pp. 48-56, 105-111.

44. F. H. Rhodes, W. H. Jones and W. R. Dougan: "The Air Slaking of Lime." Chem. & Met. Eng., 1923, vol. 28, pp. 1066-1069.

45. C. A. Jacobson (Ed.): Encyclopedia of Chemical Reactions. Vol. II. Rinhold Publishing Corp., New York, 1948, p. 137.

46. N. B. Hanny: Solid-state Chemistry, Prentice-Hall, Inc., Englewood Cliffs, New Jersey, 1967, pp. 155-157.

47. J. R. Keski and I. B. Cutler: "Initial Sintering of $Mn_xO-Al_2O_3$." J. Am. Cer. Soc., 1968, vol. 51, pp. 440-444.

48. R. D. Bagley, I. B. Cutler and D. L. Johnson: "Effect of TiO_2 on Initial Sintering of Al_2O_3." J. Am. Cer. Soc., vol. 53, pp. 136-141.

49. A. M. Alper (Ed.): High Temperature Oxide, Part III. Magnesia, Alumina, Beryllia Ceramics: Fabrication, Characterization and Properties, Academic Press, New York, 1970, pp. 129-182.

50. W. D. Kingery (Ed.): Ceramic Fabrication Processes, Tech. Press of MIT and John Wiley & Sons, Inc., New York, 1958, pp. 131-143.

51. W. D. Kingery (Ed.): Kinetics of High-Temperature Processes, Tech. Press of MIT and John Wiley & Sons, Inc., New York, 1959, pp. 187-194.

52. J. H. Brophy, R. M. Ross and J. Wulff: The Structure and Properties of Materials, Vol. II, Thermodynamics of Structure, John Wiley & Sons, Inc., New York, 1967, pp.132-144.

53. M. Timucin and A. E. Morris: "Phase Equilibria and Thermodynamic Properties of Lime-Iron Oxide Melts Containing up to 30 Percent SiO_2: 1450°C and 1550°C Sections." The Reaction Parameters of Lime, ASTM STP 472, Am. Soc. for Test. and Matl., 1970, pp. 25-31.

54. F. X. Tartaron and J. D. Ruschak: "Effect of Lime Structure on Oxygen Steelmaking." U. S. Bureau of Mines, Report of Investigation 6901, 1967.

55. K. H. Obst, J. Stradtmann and G. Tromel: "Reducing the Blowing Time in the LD Process by the Use of Special Lime Products." J. Iron and Steel Inst., 1970, vol. 208, pp. 450-445.

56. E. B. Snyder (Marblehead Lime Co.): "The Flux Story or What's with Lime in Steel's Future." Presented at March 1970 Meeting of Chicago Section, AIME-NOHC at Ill. Inst. Tech. Res. Inst.

57. G. Derge: "Discussion." The Reaction Parameters of Lime, ASTM STP 472, Am. Soc. for Test. and Matl., 1970, p. 31.

VITA

Shin Suk Kang was born on February 3, 1938, in Young-Duck, Korea. He received his primary and secondary education in Seoul, Korea. He received a Bachelor of Science Degree in Metallurgical Engineering from the College of Engineering, Seoul National University, in February 1962.

After serving in the Republic of Korea Army, he was research assistant at the Research Institute of Mining and Metallurgy, and then junior engineer at the Kwangsung Mining Company and the Korea Institute of Science and Technology.

He entered the Graduate School of the University of Missouri-Rolla in September 1967. He has been a student member of the American Society for Metals, and the Metallurgical Society of AIME.

APPENDIX A

ANALYSIS OF STARTING MATERIALS

Mallinckrodt $CaCO_3$, (Primary Standard)

Maximum limits of imputites

	%
Alkalinity	to pass test
Ammonium (NH_4)	0.003
Barium (Ba)	0.005
Chloride (Cl)	0.001
Heavy metals (as Pb)	0.001
Insoluble in HCl and NH_4OH ppt	0.005
Iron (Fe)	0.001
Magnesium (Mg)	0.01
Other alkalies	to pass test
Oxidizing substances (as NO_3)	0.005
Phosphate (PO_4)	0.001
Potassium (K)	0.01
Silica (SiO_2)	0.001
Sodium (Na)	0.0026
Strontium (Sr)	0.10
Sulfate (SO_4)	0.005
Assay ($CaCO_3$) (after 2 hours at 285°C)	99.95-100.05

Fisher Certified Fe_2O_3

Certifies of Analysis, LOT 785196

Arsenic (As)	(about 0.002%)	to pass test
Nitrate (NO_3)		0.01
Phosphate (PO_4)		0.02
Sulfate (SO_4)		0.0004
Manganese (Mn)		0.01
Copper (Cu)		0.008
Substances not ppt'd NH_4OH		0.01
Zinc (Zn)		0.002

APPENDIX B

METHOD OF CHEMICAL ANALYSIS

The well known dichromate titration method was used for the determination of the iron content in the samples. The amount of ferrous or ferric iron in a sample was not analysed individually, but total iron was determined as ferrous. All the starting materials prepared for equilibration runs were analysed in triplicate and the average value was reported. CaO was always determined by difference. The following is a brief description of the procedure. The detailed analytical procedure has been described by Timucin.[38]

About 0.4 to 0.5 gm of a dried sample (dried at 105°C for 24 hr) was placed in a tall titration beaker with 300 ml capacity and wet by 2 ml of water. About 20 ml of conc. HCl was added. The beaker was covered and gently heated. When the sample went into complete solution, all ferric ions were reduced to ferrous state by adding $SnCl_2$ solution dropwise while stirring the hot sample solution. The addition of $SnCl_2$ solution was continued until the yellow color of ferric ion just disappeared, plus one or two more drops. Then the beaker was rapidly cooled to room temperature and the solution was diluted to 150 ml. Next 10 ml of $HgCl_2$ solution, 10 ml of 1:5 H_2SO_4, and 5 ml of H_3PO_4 were added. A few drops of barium diphenylamine sulphonate (6 or 7 drops) were used as an indicator. The solution was titrated with 0.05N $K_2Cr_2O_7$ standard solution.

APPENDIX C

SUMMARY OF EXPERIMENTAL RESULTS

In Table II are listed the results obtained from the experiments on the stability region of dicalcium ferrite. The results of pellet equilibration runs are presented in Tables III and IV at 1300°C and 1400°C, respectively. Table V shows the results of hydration of pure lime and CaO-iron oxide mixtures.

In order to determine the phase boundary at a fixed pO_2, runs were made with samples of increasing amounts of "FeO" until the approximate phase boundary was determined and then repeated runs were performed to accurately confirm the phase boundary. In Tables III and IV, 3 equilibration runs which confirm the phase boundary at a fixed pO_2 are given. As mentioned earlier, the points drawn in Figs. 9 and 10 were determined based on the relative amounts of the phases present in the consecutive two samples. For example, at a given pO_2, if no liquid phase was observed in sample (a), but was observed in more than a trace amount in sample (b), and this was confirmed in repeated runs, then the phase boundary was chosen as the intermediate composition between the sample (a) and the sample (b).

Table II Experimental Results of Melting Temperature of Dicalcium Ferrite in the Presence of Excess Lime

Run No.	Gas Mixture	pO_2 (atm)	Melting Temperature Observed(°C)	Sample Condition
DF1	Air	0.21	1438	Melted
DF2	O_2/N_2 = 1/99	$10^{-2.00}$	"	"
DF3	"	"	1428	Unmelted
DF4	Pure CO_2	$10^{-2.978}$	"	Melted
DF5	O_2/Ar = 0.1/99.9	$10^{-3.00}$	"	"
DF6	"	"	1422	Unmelted
DF7	"	"	1400	"
DF8	Pure CO_2	$10^{-3.077}$	"	"
DF9	O_2/Ar = 0.01/99.99	$10^{-4.00}$	1414	Melted
DF10	"	"	1400	Unmelted
DF11	CO_2/CO = 63.83	$10^{-5.00}$	"	Melted
DF12	" = 16.03	$10^{-6.20}$	"	"
DF13	" = 7.257	$10^{-8.00}$	1300	Unmelted
DF14	" = 4.579	$10^{-8.40}$	"	"
DF15	" = 3.637	$10^{-8.60}$	"	Melted
DF16	" = 2.295	$10^{-9.00}$	"	"
DF17	" = 1.291	$10^{-9.50}$	"	"
DF18	" = 0.311	$10^{-12.00}$	1200	Unmelted
DF19	" = 0.248	$10^{-12.196}$	"	"
DF20	" = 0.177	$10^{-12.492}$	"	Melted
DF21	" = 0.115	$10^{-12.871}$	"	"
DF22	" = 0.055	$10^{-13.50}$	"	"
DF23	" = 0.31	$10^{-14.00}$	"	"

Table III Results of Equilibration Runs at 1300°C

Run No.			Gas Mixture $r=CO_2/CO$	pO_2 (atm)	Composition Weight % CaO	"FeO"	Phase(s) Observed	Holding Time(hr)
L55(a)			7.257	$10^{-8.00}$	99.0	1.0	CaO(ss)+C_2F	L55=172
L55(b)					98.5	1.5	CaO(ss)+C_2F	
L55(c)					98.0	2.0	CaO(ss)+C_2F	
L16(a)	L17(a)	L28(a)	2.295	$10^{-9.00}$	97.5	2.5	CaO(ss)	L16= 72
L16(b)	L17(b)	L28(b)			97.0	3.0	CaO(ss)+Liq.(m)	L17= 84
L16(c)	L17(c)	L28(c)			96.5	3.5	CaO(ss)+Liq.	L28=120
L24(a)	L30(a)	L57(a)	1.058	$10^{-9.673}$	97.0	3.0	CaO(ss)	L24= 84
L24(b)	L30(b)	L57(b)			96.5	3.5	CaO(ss)+Liq.(tr)	L30= 96
L24(c)	L30(c)	L57(c)			96.0	4.0	CaO(ss)+Liq.	L57=108
L25(a)	L26(a)	L31(a)	0.408	$10^{-1.50}$	96.0	4.0	CaO(ss)	L25= 72
L25(b)	L26(b)	L31(b)			95.5	4.5	CaO(ss)+Liq.(tr)	L26= 84
L25(c)	L26(c)	L31(c)			95.0	5.0	CaO(ss)+Liq.	L31= 96
L14(a)	L15(a)	L18(a)	0.248	$10^{-10.931}$	95.5	4.5	CaO(ss)	L14= 72
L14(b)	L15(b)	L18(b)			95.0	5.0	CaO(ss)+Liq.(m)	L15= 84
L14(c)	L15(c)	L18(c)			94.5	5.5	CaO(ss)+Liq.	L18= 90

(Table III continued)

Run No.			Gas Mixture $r=CO_2/CO$	pO_2 (atm)	Composition Weight % CaO	"FeO"	Phase(s) Observed	Holding Time(hr)
L22(a)	L23(a)	L27(a)	0.129	$10^{-11.50}$	94.5	5.5	CaO(ss)	L22= 72
L22(b)	L23(b)	L27(b)			94.0	6.0	CaO(ss)+Liq.(tr)	L23= 80
L22(c)	L23(c)	L27(c)			93.5	6.5	CaO(ss)+Liq.	L27= 96
L19(a)	L20(a)	L32(a)	0.112	$10^{-11.621}$	94.5	5.5	CaO(ss)	L19= 72
L19(b)	L20(b)	L32(b)			94.0	6.0	CaO(ss)+Fe(tr)	L20= 72
L19(c)	L20(c)	L32(c)			93.5	6.5	CaO(ss)+Fe	L32= 70
L33(a)	L34(a)	L35(a)	0.103	$10^{-11.70}$	95.0	5.0	CaO(ss)	L33= 78
L33(b)	L34(b)	L35(b)			94.5	5.5	CaO(ss)+Fe(tr)	L34= 72
L33(c)	L34(c)	L35(c)			94.0	6.0	CaO(ss)+Fe	L35= 97
L11(a)	L12(a)	L21(a)	0.060	$10^{-12.16}$	99.0	1.0	CaO(ss)	L11= 79
L11(b)	L12(b)	L21(b)			98.5	1.5	CaO(ss)+Fe(tr,m)	L12= 72
L11(c)	L12(c)	L21(c)			98.0	2.0	CaO(ss)+Fe	L21= 96

Table IV Results of Equilibration Runs at 1400°C

Run No.			Gas Mixture $r=CO_2/CO$	pO_2 (atm)	Composition Weight % CaO	"FeO"	Phase(s) Obsrved	Holding Time(hr)
H2(a)	H12(a)	H15(a)	10.561	$10^{-6.563}$	99.5	0.5	CaO(ss)	H2 = 24
H2(b)	H12(b)	H15(b)			99.0	1.0	CaO(SS)+Liq.(m)	H12= 30
H2(c)	H12(c)	H15(c)			98.5	1.5	CaO(ss)+Liq.	H15= 36
H5(a)	H11(a)	H20(a)	6.383	$10^{-7.00}$	99.5	0.5	CaO(ss)	H5 = 24
H5(b)	H11(b)	H20(b)			99.0	1.0	CaO(ss)+Liq.(tr)	H11= 36
H5(c)	H11(c)	H20(c)			98.5	1.5	CaO(ss)+Liq.	H20= 24
H4(a)	H9(a)	H17(a)	2.019	$10^{-8.00}$	99.0	1.0	CaO(ss)	H4 = 24
H4(b)	H9(b)	H17(b)			98.5	1.5	CaO(ss)+Liq.(tr)	H9 = 30
H4(c)	H9(c)	H17(c)			98.0	2.0	CaO(ss)+Liq.	H17= 24
H3(a)	H6(a)	H13(a)	1.058	$10^{-8.561}$	98.5	1.5	CaO(ss)	H3 = 24
H3(b)	H6(b)	H13(b)			98.0	2.0	CaO(ss)+Liq.(m)	H6 = 30
H3(c)	H6(c)	H13(c)			97.5	2.5	CaO(ss)+Liq.	H13= 30
H8(a)	H14(a)	H23(a)	0.638	$10^{-9.00}$	98.5	1.5	CaO(ss)	H8 = 24
H8(b)	H14(b)	H23(b)			98.0	2.0	CaO(ss)+Liq.(tr)	H14= 26
H8(c)	H14(c)	H23(c)			97.5	2.5	CaO(ss)+Liq.	H23= 24

(Table IV continued)

Run No.			Gas Mixture $r=CO_2/CO$	pO_2 (atm)	Composition Weight % CaO	"FeO"	Phase(s) Observed	Holding Time(hr)
H7(a)	H16(a)	H27(a)	0.202	$10^{-10.00}$	97.5	2.5	CaO(ss)	H7 = 24
H7(b)	H16(b)	H27(b)			97.0	3.0	CaO(ss)+Liq.(tr)	H16= 30
H7(c)	H16(c)	H27(c)			96.5	3.5	CaO(ss)+Liq.	H27= 28
H10(a)	H18(a)	H25(a)	0.114	$10^{-10.50}$	97.0	3.0	CaO(ss)	H10= 24
H10(b)	H18(b)	H25(b)			96.5	3.5	CaO(ss)+Liq.(tr)	H18= 24
H10(c)	H18(c)	H25(c)			96.0	4.0	CaO(ss)+Liq.(m)	H25= 27
H21(a)	H22(a)	H34(a)	0.064	$10^{-10.90}$	96.5	3.5	CaO(ss)	H21= 24
H21(b)	H22(b)	H34(b)			96.0	4.0	CaO(ss)+Liq.(tr)	H22= 26
H21(c)	H22(c)	H34(c)			95.5	4.5	CaO(ss)+Liq.(m)	H34= 30
H31(a)	H32(a)	H39(a)	0.054	$10^{-11.145}$	97.0	3.0	CaO(ss)	H31= 25
H31(b)	H32(b)	H39(b)			96.5	3.5	CaO(ss)+Fe(tr)	H32= 30
H31(c)	H32(c)	H39(c)			96.0	4.0	CaO(ss)+Fe(m)	H39= 36
H36(a)	H38(a)	H43(a)	0.045	$10^{-11.30}$	98.0	2.0	CaO(ss)	H36= 26
H36(b)	H38(b)	H43(b)			97.5	2.5	CaO(ss)+Fe(tr)	H38= 32
H36(c)	H38(c)	H43(c)			97.0	3.0	CaO(ss)+Fe(m)	H43= 24

(Table IV continued)

Run No.			Gas Mixture $r=CO_2/CO$	pO_2 (atm)	Composition Weight % CaO	"FeO"	Phase(s) Observed	Holding Time(hr)
H40(a)	H41(a)	H46(a)	0.036	$10^{-11.50}$	99.5	0.5	CaO(ss)+Fe(tr or m)	H40= 28
H40(b)	H41(b)	H46(b)			99.0	1.0	CaO(ss)+Fe(m)	H41= 24
H40(c)	H41(c)	H46(c)			98.5	1.5	CaO(ss)+Fe	H46= 36

Table V Hydration of Lime and Lime-Iron Oxide Mixtures

Sample No.	Sintering Temperature	Pellet Composition	Initial Weight	% $Ca(OH)_2$ Formed After Times of Hydration						
				2 hr	5 hr	13 hr	24 hr	36 hr	60 hr	84 hr
S1-1		Pure lime	0.980	3.72	6.48	12.62	22.57	35.41	76.07	102.29
S1-2		1½% "FeO"	0.980	1.37	3.21	6.46	10.91	17.81	34.29	51.97
S1-3	1200°C	4% "	1.021	0.00	0.43	1.47	2.93	4.21	6.96	10.20
S1-4		8% "	0.900	0.80	0.87	0.95	1.21	1.35	1.77	1.94
S1-5		12% "	0.857	0.00	0.00	0.00	0.00	0.00	0.00	0.00
S2-1		Pure Lime	0.993	4.46	8.47	11.93	27.31	40.68	76.18	101.63
S2-2		1½% Fe_2O_3	0.950	0.79	0.95	1.80	3.61	5.61	9.08	11.41
S2-3	1400°C	4½% "	0.654	1.05	1.14	1.76	3.19	4.71	7.81	10.33
S2-4		9% "	0.910	0.45	0.79	1.95	4.18	6.30	9.79	14.96
S2-5		13% "	0.744	0.88	1.34	2.52	4.44	6.41	9.60	14.00
S3-1		1½% Fe_2O_3	0.954	0.78	0.82	1.14	1.93	2.71	4.28	5.45
S3-2	1450°C	4½% "	0.915	0.85	1.02	1.60	2.76	3.99	6.58	8.49
S3-3	(Slow Cooled)	9% "	0.899	0.76	0.76	0.83	0.87	0.90	1.01	1.01
S3-4		13% "	0.759	0.62	0.66	0.74	0.82	0.94	1.11	1.19
S4-1		1½% Fe_2O_3	0.945	1.29	1.75	2.67	3.66	4.52	6.10	7.68
S4-2	1450°C	4½% "	0.837	1.12	1.23	1.60	2.23	2.64	3.68	4.50
S4-3	(Quenched)	9% "	0.889	0.84	0.84	1.05	1.40	1.86	3.37	5.47
S4-4		13% "	0.834	1.05	1.46	2.46	4.29	6.87	12.62	18.63

(Table V continued)

Sample No.	Sintering Temperature	Pellet Composition	% $Ca(OH)_2$ Formed After Times of Hydration						
			108 hr	132 hr	154 hr	176 hr	241 hr	313 hr	481 hr
S1-1		pure lime	110.01	112.40	113.45	114.15	114.94	115.47	116.12
S1-2		1½% "FeO"	63.10	70.80	77.39	81.68	82.53	84.11	86.80
S1-3	1200°C	4% "	13.89	17.89	22.50	27.84	43.71	53.14	69.48
S1-4		8% "	2.29	2.56	2.60	2.84	3.39	3.57	4.50
S1-5		12% "	0.00	0.00	0.00	0.00	0.00	0.00	0.00
S2-1		pure lime	109.51	111.90	113.06	113.84	114.56	116.15	117.45
S2-2		1½% Fe_2O_3	14.07	18.43	26.07	36.43	74.69	90.13	100.85
S2-3	1400°C	4½% "	14.23	21.04	30.84	41.55	66.87	79.11	95.33
S2-4		9% "	22.36	33.07	45.19	56.04	76.38	83.77	92.91
S2-5		13% "	21.33	32.52	44.80	56.41	78.29	85.75	93.71
S3-1		1½% Fe_2O_3	6.60	7.41	8.26	9.27	23.54	37.43	80.41
S3-2	1450°C	4½% "	10.53	14.18	20.79	31.08	63.19	76.14	94.79
S3-3	(Slow Cooled)	9% "	1.11	1.14	1.18	1.28	9.35	9.39	12.86
S3-4		13% "	1.31	1.85	2.01	2.75	9.61	24.51	64.74
S4-1		1½% Fe_2O_3	10.39	14.74	21.30	30.37	58.95	72.40	89.48
S4-2	1450°C	4½% "	5.69	7.33	10.09	14.59	37.33	42.99	67.03
S4-3	(Quenched)	9% "	8.63	12.62	17.95	25.04	36.26	49.86	70.20
S4-4		13% "	24.35	30.84	36.59	42.57	60.64	70.99	86.03